ABSTRACT

FEASIBILITY OF LOW ENERGY PLASMA TORCH FOR

REACTION CONTROL THRUSTER IGNITION

By

Chunyoung Park

May 2015

A DC–thermal plasma jet is proposed as a reliable ignition source for reaction control system (RCS) thrusters employing oxygen with hydrocarbons, like methane. Industrial plasma torch systems are analyzed to understand the behavioral characteristics of DC–thermal plasmas. Nitrogen is used as a working gas for the source of plasma jet to understand the general mechanism of thermal plasma formation. DC–thermal plasmas require high electrical energy to maintain their arc discharge status which presents challenges in space systems. The purpose of this study is, therefore, to find a suitable configuration which minimizes power consumption.

Various physical and electrical conditions relate to a thermal plasma formation. In this study, the input voltage (221–332V) and pressure (5–15 psi) are applied as initial conditions. The DC–power module and starter module are designed as plasma drivers and a commercial off–the–shelf torch head is used for this research. The normalized method is developed to estimate the arc temperature. Test results show that the lowest

power consumption and arc–starting voltage are 1,321W and 248.8 VDC, respectively. In addition, it is found that the current is a major factor for varying the mass flow rate.

Since the lowest power consumption is still high, future improvements and research should focus on integrating a high–power and lightweight energy source, developing a high–frequency and half–duty cycle power system, and incorporating a composite cathode. In addition, a new conceptual torch design is proposed to be considered as an igniter for RCS thrusters. The next step would be to repeat the plasma torch tests with the new configuration at ambient and vacuum conditions. These would be followed by combustion tests to verify the actual functionality of the plasma igniter for RCS thrusters with various oxidizer and fuel mixture ratios. In parallel, research should focus on miniaturization of the electrical system.

FEASIBILITY OF LOW ENERGY PLASMA TORCH FOR REACTION CONTROL THRUSTER IGNITION

A THESIS

Presented to Department of Mechanical and Aerospace Engineering

California State University, Long Beach

In Partial Fulfillment

of the Requirements for the Degree

Master of Science in Mechanical Engineering

Committee Members:

Eric Besnard, Ph.D.
Hsun Hu Chen, Ph.D.
Mark Holthaus, M.S.

College Designee:

Antonella Sciortino, Ph.D.

By Chunyoung Park

B.S., 2010, Yonsei University

May 2015

ACKNOWLEDGEMENT

First and foremost, I would like to thank God for his daily inspiring involvement. Without His support, I would have never made it to the point where I am at today. I would also like to thank my advisor, Dr. Eric Besnard, for his guidance and support throughout my graduate years at California State University, Long Beach. For the past three years, I have not only gained academic knowledge of propulsion and space systems but also learned the actual methodology of rocket engine testing and numerous hands–on experiences through working with him. I would like to express my sincere appreciation and respect to him for giving me the opportunity to research fluid and electric systems which have practical relationships in the aerospace industry. In addition, I would like to thank him for providing me with mentors who gave me helpful technical suggestions. I would like to thank Xavier Rogers for his time and efforts in assembling parts and sharing his ideas to solve technical problems. I also would like to extend my thanks to my mentor, Mark Holthaus, for his assistance with electrical and mechanical system design. My thanks also go out to all of my friends who have believed in me and encouraged me to move forward over the years.

Lastly, but definitely not least, I would like to thank my parents for their encouragement throughout my studies. Without their support and love through the difficult times of the M.S. process, it would have been much harder to bear.

TABLE OF CONTENTS

CHAPTER Page

LIST OF TABLES

TABLE Page

LIST OF FIGURES

FIGURE Page

CHAPTER 1

INTRODUCTION

According to the Federal Aviation Administration's commercial space transportation forecasts, the demand of suborbital reusable vehicles (SRV) has been increasing for research, commercial, and educational purposes [1]. In addition, NASA also decided to develop a methane/LOX rocket engine for the lunar and deep space mission [2] and SpaceX confirmed in October 2013 that they intend to build a family of methane–based Raptor rocket engines [3]. The characteristic of the new generation vehicles is that their propulsion system requires several on/off cycles for their main engine and numerous ones for the reaction control system (RCS) thrusters [4]. Unlike conventionally used storable propellants, methane and oxygen are not hypergolic and require a separate ignition source. Spark and glow plug ignition systems have been researched and used for a bi–propellant propulsion system [5–8]. However, the spark igniter system requires two additional feed lines for each thruster and other features such as a combustion chamber, an injector, and electrodes to make combustion gas ignite a larger scale thruster. This will result in overall weight increase for the space vehicle and make the engine configuration and feed system more complex. In addition, the presence of unreliable operation for the spark igniter exists due to the varying propellant temperatures and environmental conditions including vacuum of space. On the other hand, the glow plug igniter has a relatively simpler configuration than spark igniter.

However, the ignition delay is much longer than spark plug (7–11s); therefore, it is not suitable for quick operation. One remedy was proposed to solve this issue. The remedy is to maintain the glow plugs to be powered up before the engine sequence begins, so that quick ignition is possible. However, emergency RCS operations may sometimes be necessary due to an unexpected situation. In this case, maintaining the temperature of the glow plug is necessary for entire period of mission. This results in a significant power loss for the space vehicle.

According to a recent study [9], plasma assisted combustion systems have been researched for scramjet engines due to its high reliable and repeatable capability in challenging combustion conditions. Moreover, research [10] shows the possible applications for aerospace vehicles and practical size of the plasma igniter system (See Figure 1). For this research, industrial plasma torches are investigated as a possible ignition system for the next generation of RCS thrusters.

FIGURE 1. Combined cycle plasma torch in operation [11].

Industrial plasma torches are widely used for various manufacturing applications such as plasma coating, welding, and cutting [12]. Due to the high temperature characteristic of thermal plasma, the plasma torches are mainly used for metal processing. The temperature of the thermal plasma is around 2,000K–25,000K depending on the type of working gas and input power setting. The main contribution for the temperature of the thermal plasma is electric power. However, the overall input power does not meet the starting condition for the thermal plasma.

In this research, open circuit voltages and overall power consumption are investigated to provide the electrical conditions for future development. In addition, helium, argon, carbon dioxide, oxygen and nitrogen gases are used as a working gas. In particular, helium, oxygen, methane and sometimes nitrogen gases are available in liquid propulsion systems; as such they can be the source of working gas for thermal plasma for the ignition system of the thrusters. For this research, nitrogen gas is used as a working gas and extensions of the research would address other gases for future practical applications.

CHAPTER 2

LITERATURE REVIEW AND INTRODUCTION TO PLASMA TORCHES

Introduction to Plasma Physics

Electric discharges can be divided into four areas depending on their physical and electrical characteristics (See Figure 2). The Townsend discharge has a very weak current, so the discharge region remains dark. The glow discharge has low current, high voltage and low pressure. In glow discharge, the plasma is weakly ionized and starts glowing. The corona discharge has low current at atmospheric pressure. The arc discharge has high current and low voltage at atmospheric pressure. In arc discharge, the plasma emits a large amount of light and can be considered as a state of thermodynamic equilibrium. This is the area that this research focuses on because the plasma has high enthalpy and can therefore deliver large energy to the propellants for reliable ignition [13].

Local Thermodynamic Equilibrium (LTE)

According to the definition of thermodynamic equilibrium (TE), all species of particles such as electrons, neutral atoms, ions, and molecules are considered to have the same temperature in the system. Complete thermodynamic equilibrium (CTE) corresponds to the case where all particles have uniform temperature distribution within an entire region of the system. In plasma systems, CTE represents a homogeneous temperature distribution for all degrees of freedom and all of their possible reactions.

However, the CTE condition is hardly achievable for real systems. Therefore, a more realistic method for approximating CTE is called local thermodynamic equilibrium (LTE) [14]. Local thermodynamic equilibrium (LTE) is an assumption that the thermodynamic equilibrium is achievable for all thermodynamic properties in a small domain at the local values of temperature and pressure.

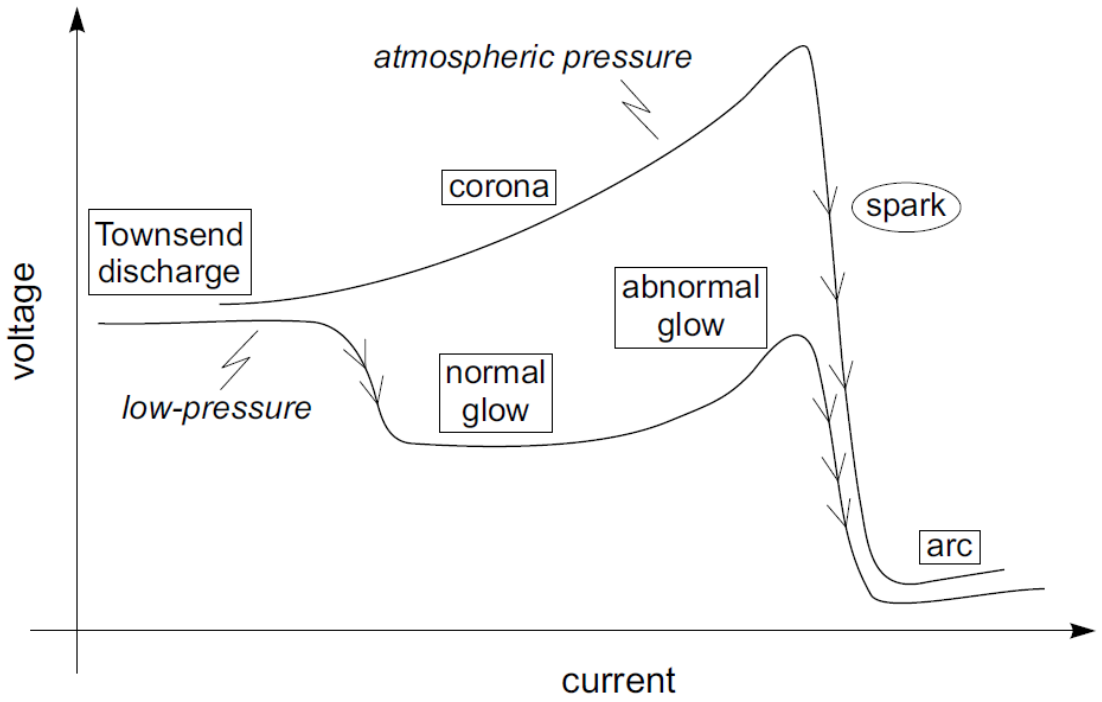

FIGURE 2. Voltage–current characteristics of the different types of discharges in gases [13].

Plasma Torch Design

Configurations

A plasma torch has two separate sections which are the body and the electrode. The torch body is a structure that holds the electrode configurations and connects with

other assemblies (See Figure 5). In addition, the torch body becomes a chamber that holds the pressure of working gas. The electrode configuration consists of two parts which are called anode and cathode. In general, the cathode is made of a heat–resisting material to increase its life [15].

Classification based on Operating Mode

Plasma torches can be categorized in two different arc–generation modes which are transferred and non–transferred modes. In the transferred mode, the arc is electrically transferred to a target. In the non–transferred mode, the arc is electrically transferred between torch electrodes and blown out to a target (See Figure 3).

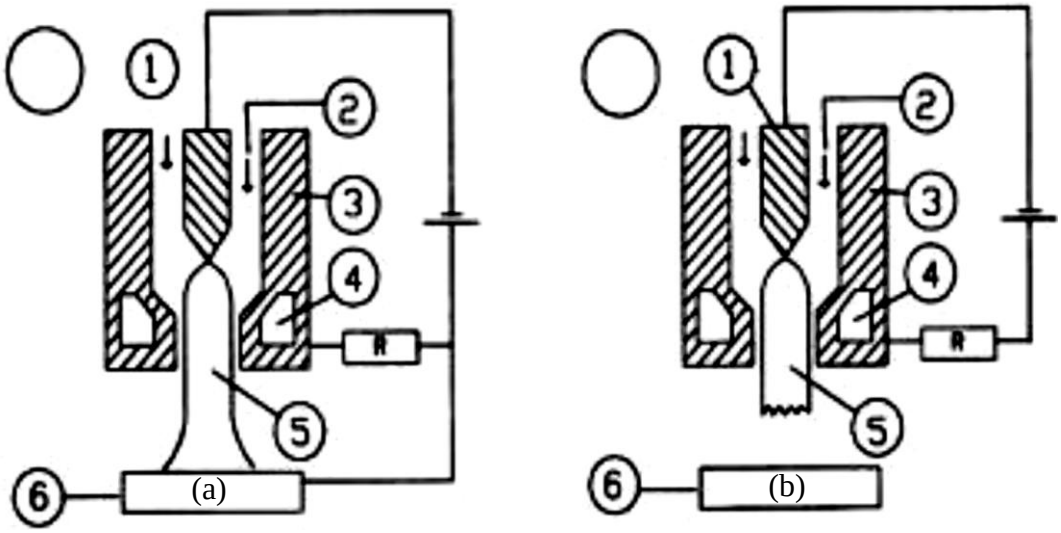

FIGURE 3. Operation modes for plasma torches. (a) transferred and (b) non–transferred arc mode of operation. 1, Cathode; 2, Gas Flow; 3, Anode; 4, Cooling Channel; 5, Plasma Jet; 6, Substrate [12].

The transferred plasma torch creates a plasma arc directly between the cathode and a target. To accomplish this condition, the main power module needs to be

connected to the target and cathode [12]. The body structure of the torch holds the cathode and provides a separation of the secondary electrode which is connected to a high voltage ionization module and, depending on the electrical system design, a cooling or shielding gas nozzle. The non–transferred plasma torch creates a plasma arc between the cathode and anode. However, both electrodes are enclosed in a single structure assembly [12].

Industrial Plasma Torch

Metal processing technology has been developed and plasma technology has been noticed as a new advanced method due to its high temperature characteristic. Thermal plasmas are the gases that are ionized with the electric discharge and the gases are characterized by a high temperature (2,000–20,000K). Since the thermal plasma has an extremely high temperature, it has the outstanding capability to cut or weld metals.

The performance of the plasma torch is determined by the combination of electrical power and mass flow rate. If the mass flow is not dense enough to transfer heat to the target, or if the electric power is not enough to ionize the working gas, the expected torch performance cannot be achieved for its purpose. Therefore, Venkatramani [12] showed a voltage–current diagram for industrial plasma torches and summarized their power consumption and applicable fields. The voltage–current diagram also shows the power range of industrial plasma torches according to the arc–generation mode. In addition, table 1 shows the voltage range depending on the type of working gas the and arc–generation mode. These two results present the approximation of the maximum available power range for the research. The goal of this research is to generate thermal plasma and minimize the power consumption for the electrical system.

According to the figure 4, the appropriate power consumption range which also satisfies minimum arcing conditions is somewhere between 100–2,000W.

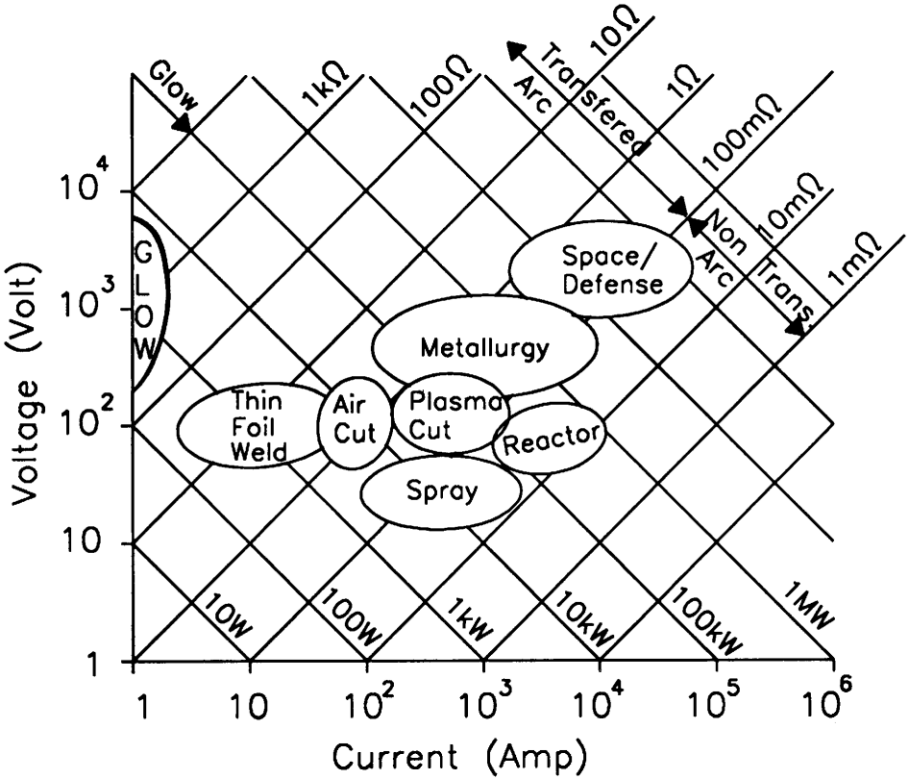

FIGURE 4. Voltage–current diagram for plasma torches [12].

Geometric Configuration of Plasma Torch and Performance

The geometric dimensions of plasma torches are an important factor because they affect the operational stability and power consumption of the plasma torch significantly. Two electrodes, which are called anode and cathode, are required to generate DC–plasma in general. In addition, a flow swirler is an important part for the torch assembly (See Figure 5). The power consumption and arc stability are related to the electrode gap distance and the throat–diameter of the nozzle [16].

TABLE 1. Arc Voltages (Volts) in the Cutting and Spraying Applications [14]

Gas	Transferred arc mode (cutting)	Non–transferred arc mode (spraying)
Argon	110–300	25–50
Nitrogen	150–400	60–100
Argon/hydrogen	130–350	80–100
Nitrogen/hydrogen	150–400	90–150

Electrodes

Electrodes consist of anode and cathode. Anode is normally made of copper due to the high electron emissivity and effective cooling. The anode is electrically charged as positive and becomes a nozzle of the torch assembly. Cathode is made of a high heat resistance material such as tungsten. Cathode is electrically charged as negative and normally located in the center of the torch assembly [16].

Flow Swirler

A flow swirler is a component that changes an incoming axial flow to a vortex flow. There are several benefits using a swirler for plasma torches. First of all, a vortex flow concentrates the arc on the center of the anode throat. Therefore, the plasma jet becomes more stable. In addition, the vortex flow provides cooling to the anode, so electrode erosion is also reduced [16].

Electrodes Gap

The distance between the electrodes is the place where the plasma arc is generated. A high electric field ionizes the working gas and the ionization voltage is dependent on the gap distance. As shown in figure 6, the voltage requirement is

proportional to the arc gap. Therefore, the electrode gap is a significant factor for both thermal plasma generation and total power consumption [16].

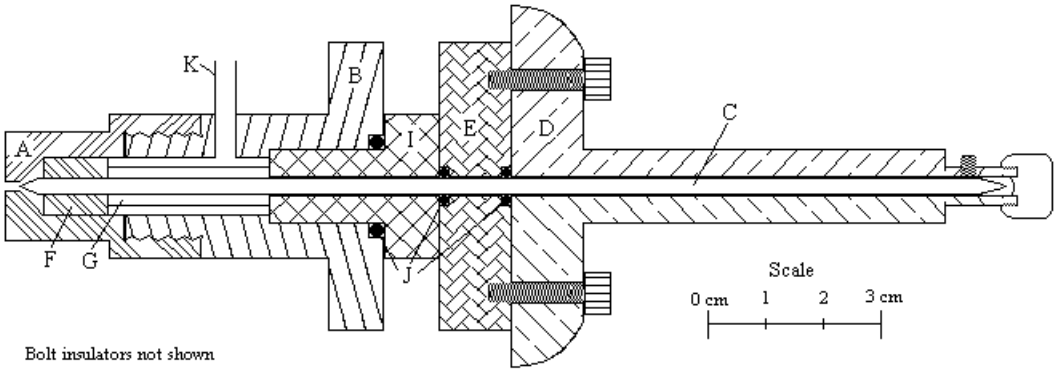

FIGURE 5. Example of plasma torch assembly. A: Anode, B: Torch body, C: Cathode, D: Micrometer drive, E: Cathode bracket, F: Flow swirler, G: Support rod, H: Bolt jackets, I: Body insulator, J: O–rings, K: Feedstock lines [15].

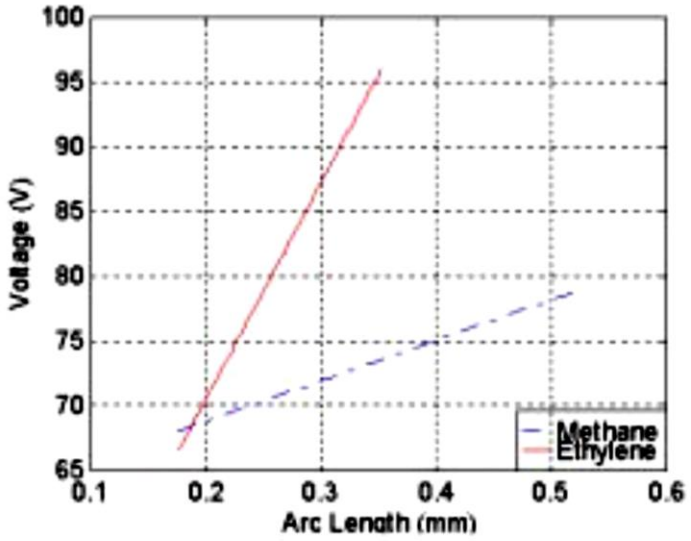

FIGURE 6. Arc gap influence on input voltage. Every test was run at 30 SLPM (or about 1.72-2.07 MPa in the gas line) with either methane or ethylene and at constant DC current. Initially the plasma torch was set to its normal 0.178 mm arc gap and run at approximately 25 A [16].

Temperature Analysis of Plasma Arc

In general, the temperature of the thermal plasma is high, but their temperature profiles differ by the type of working gas. In addition, the temperature profiles can be altered by physical parameters such as electrical input power, mass flow rate, and geometry of the torch nozzle. Since the temperature of the arc has a direct effect on the combustion, investigation of the temperature of the arc column is essential. However, both mass flow rate and input power affect the overall arc temperature; therefore, normalization for the power is used in the analysis. The normalized power is defined to be the fraction of power over mass flow rate. Using this definition, it is possible to determine how the input power affects the temperature and overall temperature range with the same mass flow rate for various types of working gas.

The data for mass flow rate and temperature was obtained from both experimental and theoretical studies [17–23] with the arc temperature recorded at a point near the nozzle. Figure 7–9 shows that the data points for the temperature can be grouped by the type of working gas. The average temperature of oxygen and oxygen–nitrogen mixed plasma group is about 26,700K and the average temperature of the argon plasma group is about 13,500K. Moreover, the temperature of argon and oxygen–nitrogen plasma increases slightly when the normalized input power increases. However, there is a limitation that temperature does not exceed for each group. This result gives an important insight that even though the same amount power is consumed, the arc temperature is highly dependent on the type of working gas. In addition, increasing input power also increases the arc temperature among the same group. From

these results, the thermal plasma arc with nitrogen and oxygen gas has the capability to make combustion for propellant mixtures.

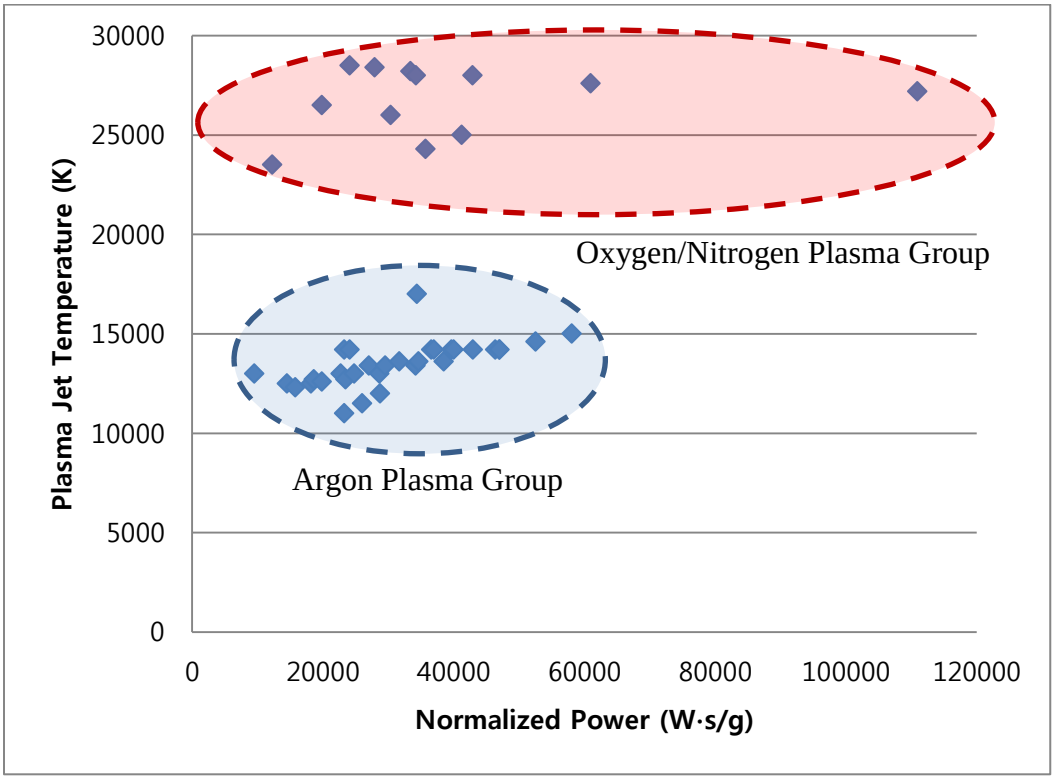

FIGURE 7. Plasma jet temperature vs. normalized power.

Input Power Influence on Mass Flow Rate

According to previous research [17], the increase of power consumption for arc discharge can also increase the chamber pressure at the same mass flow rate. This is due to the fact that, as the gas flows and becomes a plasma jet by electric discharge, the temperature drastically increases which is considered to be the same effect as the throat restriction; therefore, it leads to higher chamber pressure. In addition, the isentropic flow

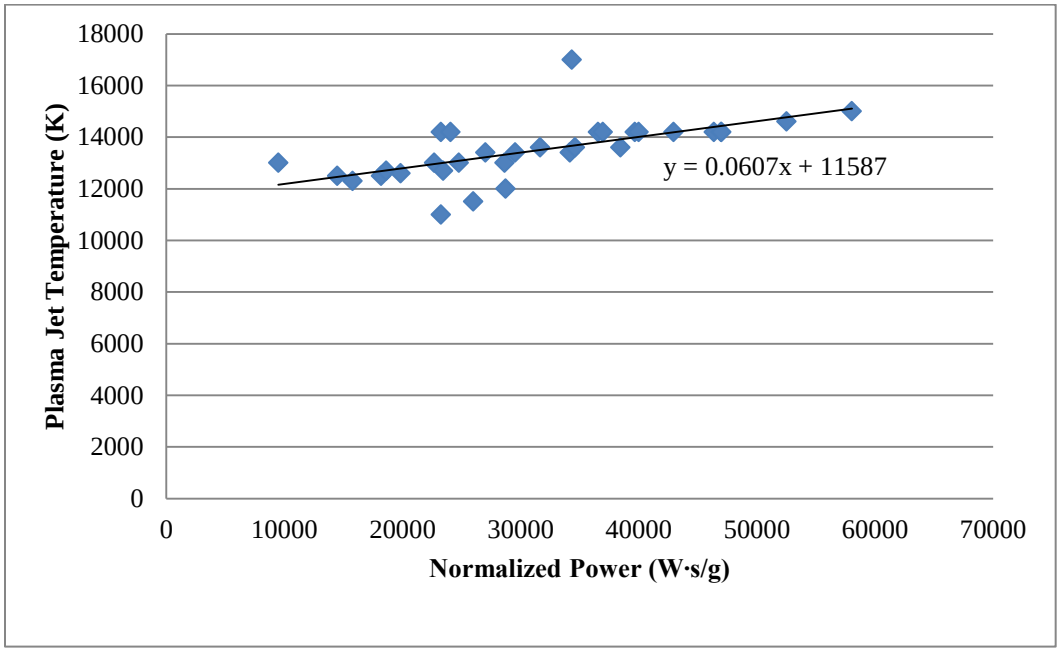

FIGURE 8. Argon plasma temperature vs. normalized power.

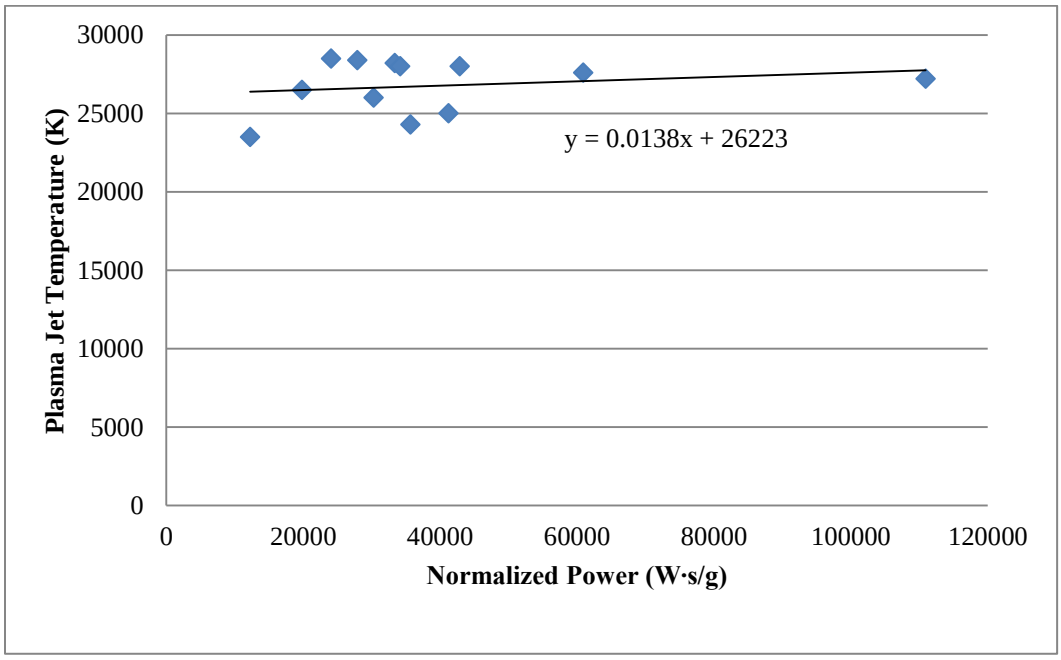

FIGURE 9. Oxygen and nitrogen plasma temperature vs. normalized power.

equation indicates that the temperature increases lead to the decrease of the mass flow rate if chamber pressure is fixed. The isentropic flow equation is as follows:

$$\dot{m} = \frac{p_0 A^*}{\sqrt{T_0}} \sqrt{\frac{\gamma}{R}\left(\frac{2}{\gamma+1}\right)^{(\gamma+1)/(\gamma-1)}}$$

where:

$\dot{m}$ = Mass flow rate

p_0 = Gas chamber pressure

T_0 = Gas chamber temperature

γ = Specific heat ratio

R = Gas constant

However, the heat capacity at constant pressure (C_p) and the heat capacity at constant volume (C_v) are not known at an extremely high temperature; therefore, the isentropic flow equation is not applicable for thermal plasma flows.

Table 2 shows the relationships between input power, chamber pressure, mass flow rate, and nozzle diameter. These data points are useful to find out how the input power and chamber pressure are related with a fixed nozzle diameter. Especially, the first three rows have the same mass flow rate while chamber pressures and input power are different. From these results, it is clear that an input power increase raises the chamber pressure with the same mass flow rate. However, general compressible gas flow equations cannot be applied to calculate the mass flow rate due to the unknown density for the working gas at an extreme temperature. The alternative method for the mass flow calculation is proposed in chapter 3.

TABLE 2. Operational Condition for Oxygen Plasma Torch [17]

Voltage (V)	Current (A)	Power (W)	Pressure (atm)	Mass Flow(g/s)	Nozzle Diameter(mm)	Normalized Power (W ·s/g)
114	100	11,400	1.78	0.93	2	12,258
123	150	18,450	2.07	0.93	2	19,838
159	200	31,800	4.15	0.93	2	34,193
132	200	26,400	2.47	0.238	2	110,924
145	200	29,000	3.15	0.476	2	60,924
153	200	30,600	3.74	0.714	2	42,857
159	200	31,800	4.24	0.952	2	33,403
166	200	33,200	4.79	1.19	2	27,899
172	200	34,400	5.32	1.429	2	24,072

Final Remarks

Since DC–thermal plasma has high temperature characteristics, it can be used for an ignition source for RCS thrusters. Therefore, the goal of this research is to find out the electrical conditions that satisfy the lowest power consumption while maintaining its ignition capability. To generate thermal plasma, a DC–power module, starter module and torch head assemblies are necessary. In chapter 3, the designs of the experimental apparatus are introduced for the research.

CHAPTER 3

EXPERIMENTAL APPARATUS

There are numerous studies on sustaining conditions of thermal plasmas but only a few on the analysis of the staring conditions, sometimes referred to as initiation. This is due to the fact that for industrial applications, most of the power is used during sustained torch operations, but when the torch is used for ignition applications, the duration of the entire sequence of plasma torch operations lasts only a few milliseconds, possibly up to 100 ms. As a result, the plasma initiation phase is important and must be well understood in order to optimize the system.

In industrial plasma torch applications, pilot arc and blowback methods are widely used for plasma torch initiation. The pilot arc method requires a starter module to initiate a process of arc discharge. For this method, the design of the torch head becomes simple, and thermal plasma can be generated with a relatively low chamber pressure (30–35 psi). On the other hand, the blowback method initiates the arc discharge by mechanically contacting and releasing the electrodes. In that case, issues associated with a high voltage and associated electromagnetic interference (EMI) are minimal. However, the design of the torch head is mechanically complex and a relatively high pressure (80–110psi) is required for the chamber. Eichholz [24] published a plan of the electrical system for a plasma cutter. His design uses the pilot

arc method for starting DC arc discharge. The electrical systems for this research are designed based on this approach.

Plasma Torch Head Configuration

The head of the plasma torch is the location where the plasma arc is produced. The basic configuration of the torch head is shown in figure 10 and is comprised of electrodes, a body structure, and a flow swirler. The geometries and dimensions of each part affect the performance and stability of the system. For this research, a "PT–31 plasma torch head" is used. The PT–31 torch head, originally designed as a transferred type, consists of a shielding cap, flow swirler, nozzle, and cathode. The benefits of using an existing plasma torch are reduced manufacturing costs and high functional reliability of the electrode and swirler. For the test setup, the high voltage wire is connected to the nozzle tip, and cathode is connected to the negative output of DC–power module. Since the PT–31 is designed as a transferred type, a tungsten rod is placed in front of the nozzle exit and connected to the positive output of DC–power module (See Figure 11).

FIGURE 10. PT–31 torch head components. A: Shielding cap, B: Flow swirler, C: Nozzle, D: Cathode. Shielding cap holds all the components in place. Flow swirler changes an incoming axial flow to a vortex flow. Nozzle constricts the flow. Cathode is a terminal that produces electrons.

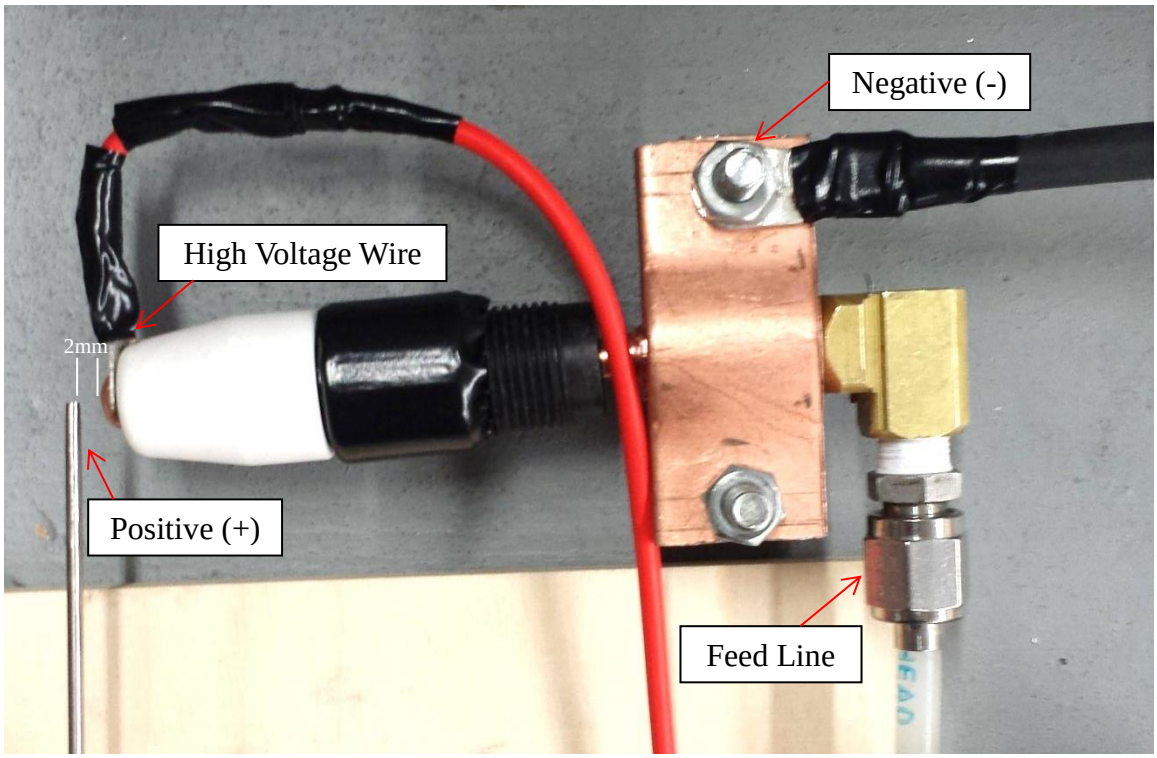

FIGURE 11. Test–setup configuration for torch head. The high voltage wire is connected to the nozzle and the cathode has a connection with the feed line. The negative wire is connected to the feed line.

Flow System

The concept of the plasma igniter system is to make combustion for starting a rocket thruster through thermal plasma. Therefore, the thermal plasma must be generated in a short time and injected into the combustion chamber while it maintains a high temperature (See Figure 12). Since the thermal plasma is constantly injected into the chamber, the right amount of working gas is also constantly supplied (See Figure 13). For this research, a flow system is designed to provide nitrogen gas to the torch head, and a solenoid valve (MAC Series 35) is installed to control the gas flow. In addition, two pressure transducers (Omega PX480A–1KSV) are also installed on the upstream and

FIGURE 12. Schematic diagram for composition process with plasma jet injection.

downstream sides of the control valve to estimate the chamber pressure of the torch and calculate the mass flow rate of the working gas. Figure 13 shows the fluid schematic of the plasma igniter system. The mass flow rate can be calculated from the gas flow formula with the known valve flow coefficient (C_v). Since the diameter of the nozzle is 1 mm and thermal plasma is also generated, the gas flow is choked at the nozzle. Therefore, the pressure difference between the upstream and downstream sides at the valve is not significant. The C_v value of the MAC Series 35 solenoid valve is 0.15. The constant gas temperature (300K) is assumed since the gas is stored at room temperature and mass flow rate is very low. The gas flow formula for low–pressure differential flow [25] is as follows:

$$Q = 16.05\, C_v \sqrt{\frac{P_1^2 - P_2^2}{(SG)\, T}}, P_2 > \frac{P_1}{2}$$

where:

C_v = Valve flow coefficient

Q = Volume flow rate in SCFM

P_1 = Inlet pressure in PSIA

P_2 = Outlet pressure in PSIA

SG = Specific Gravity

T = Temperature of gas in Degree Rankine

Data Acquisition System

The data acquisition and control (DAQ) system is designed to control the fluid and electrical systems, and collect pressure and current data during the experiments. An analog input module (NI 9201, 8 Ch, ±10 V, 500 kS/s, 12-Bit C Series) is used to measure the current with a current probe (Agilent 1146a AC/DC). A sourcing digital output module (NI 9474, 8 Ch, 5 to 30 V, 1 μs Sourcing C Series) was used to control the MAC solenoid valve. An analog input module (NI 9205, 32 Ch, ±200 mV to ±10 V, 16-Bit, 250 kS/s C Series) was used to collect the data from the pressure transducers. In addition, LabVIEW software was developed to control the DAQ system and process the data from the sensors. Since the LabVIEW software is capable of collecting 1000 samples in a second, all pressure and current data are saved with millisecond accuracy. A Fluke 179 True RMS Digital Multimeter was used for measuring DC output voltage (VDC) from the DC power module and AC output voltage (VACrms) from the variable transformer. A low–pass filter was designed and installed to improve the accuracy of voltage signals from the pressure transducers and the current probe. In addition, a 500W isolation transformer was used to block high voltage noise from the AC power for the DAQ system and the control computer (See Figure 14).

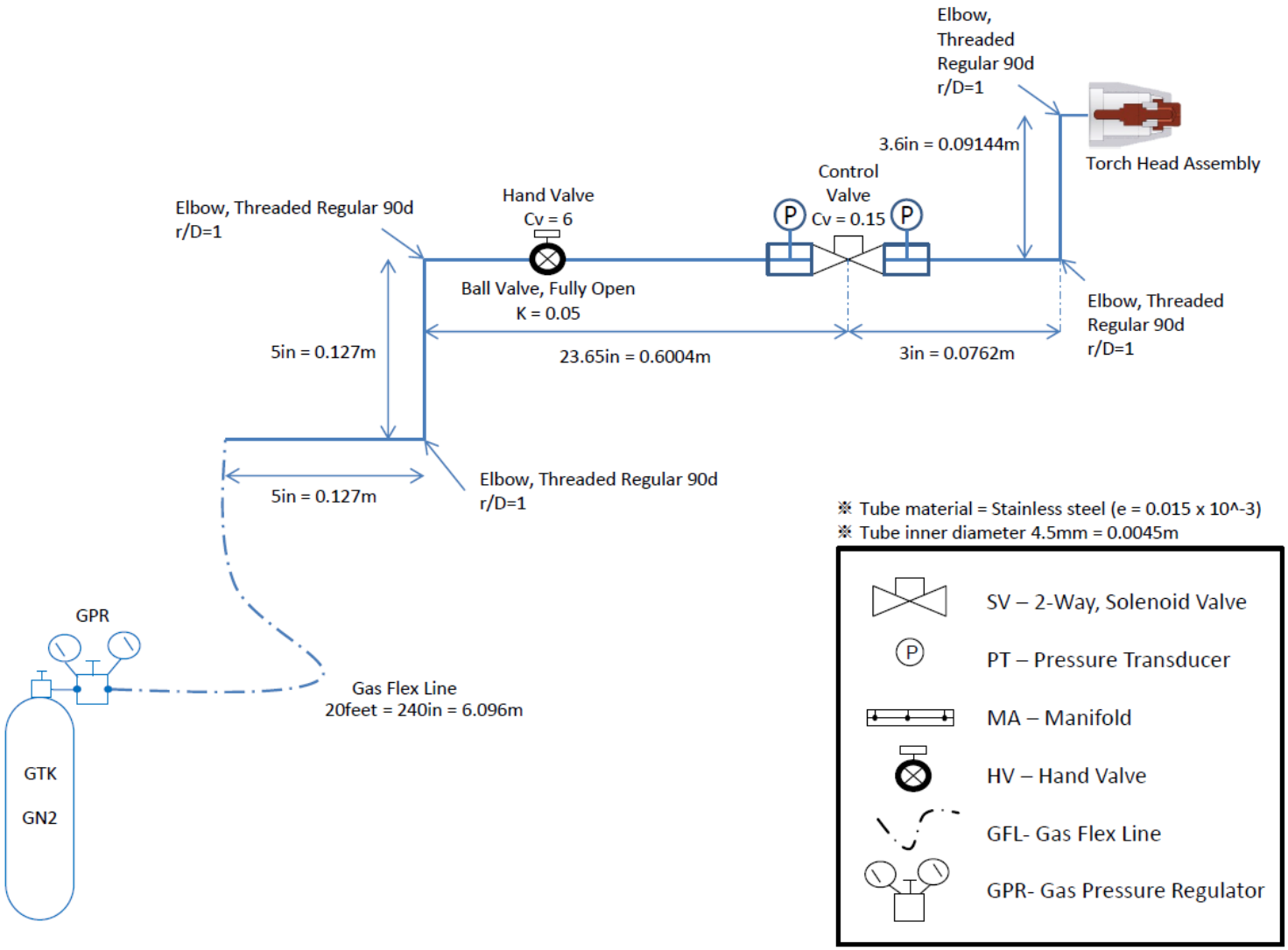

FIGURE 13. Fluid schematic of plasma igniter system.

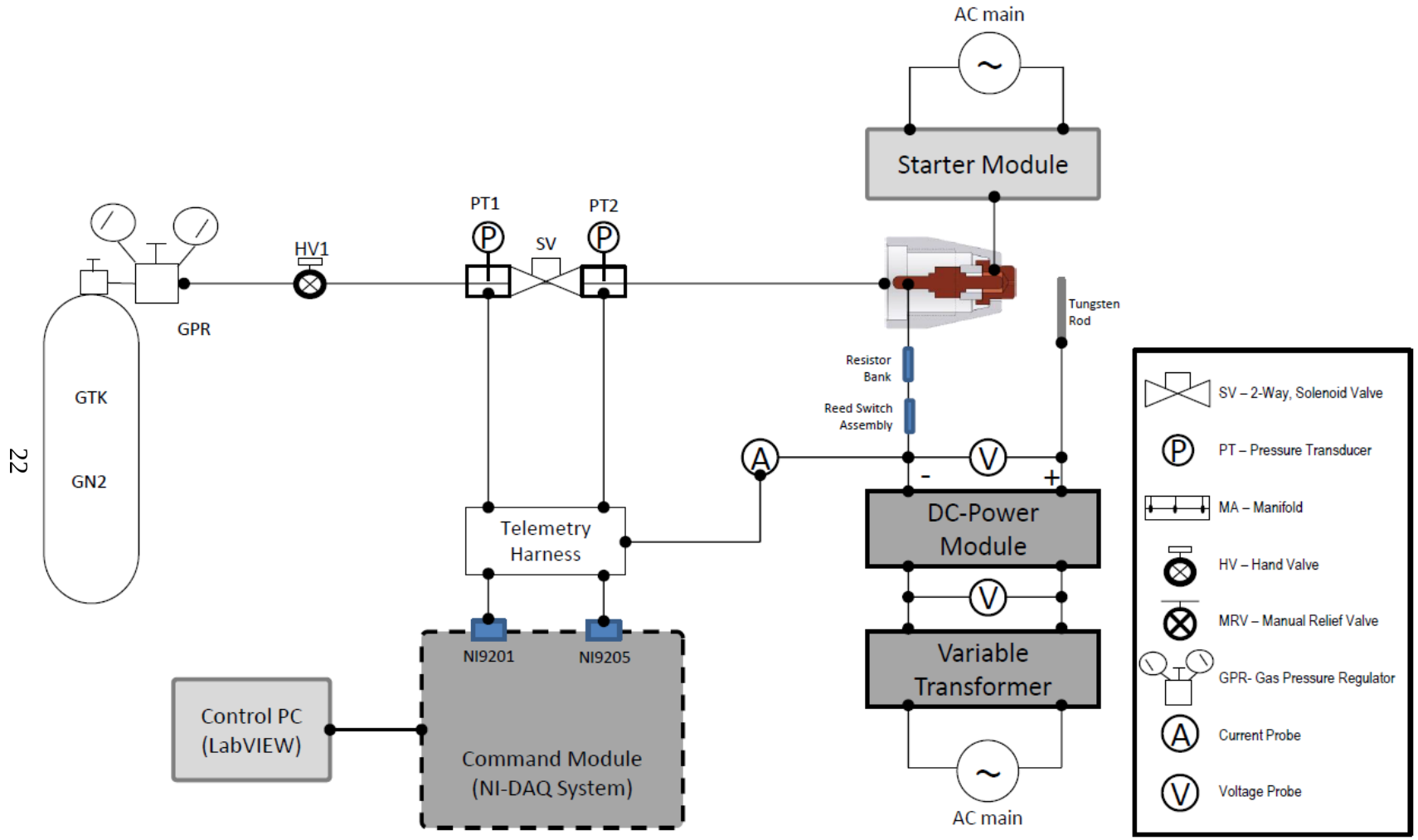

FIGURE 14. Schematic diagram for data acquisition system.

DC–Power Module

The DC–power module is a device which supplies low voltage and high current for the plasma torch to create thermal plasma (See Figure 15). For industrial plasma torch applications, the power modules have various output voltages and current capabilities depending on the purpose. However, since the aim of this research is to seek the minimum power consumption achieving thermal plasma, the DC output voltages from the power module are limited to less than 400V. For this research, the power source is 125VAC from a wall outlet, and the total output power is limited to the maximum allowable AC wall power.

The DC–power module consists of a 120VAC 40A 2 pole contactor, a 1000V–50A full bridge rectifier, and two 400VDC–2500uF electrolytic capacitors (See Figure 15). The function of the contactor is to turn the module on or off. The 2500uF capacitors are selected to provide a constant DC output voltage while thermal plasma is being generated, but the capacitance is subject to change for the new future application in order to optimize the size of the electrical system. In addition, a special feature of the power module is a voltage–doubler circuit. The voltage–doubler circuit is designed to produce doubled DC–output voltage. Appendix A shows the electric schematic of the doubler circuit. The voltage–doubler has an important role because the arching process may not occur with a very low voltage. The rated output voltage from the AC wall power is 125V. Therefore, the maximum DC voltage from the power module is limited to 340VDC. A 130V–10A variable transformer is installed to control the input AC voltage for the DC–power module. The variable transformer is a device that provides a

variable AC output voltage. For safety reasons, the output voltage from the variable transformer must not exceed the rated voltage of the electrolytic capacitors.

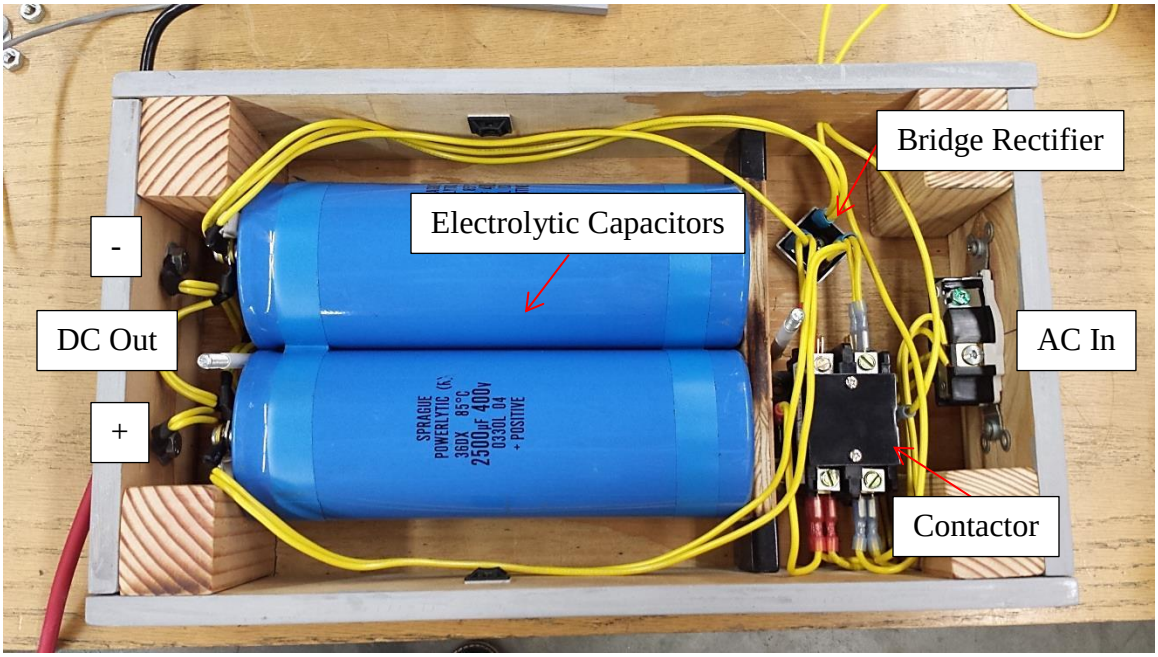

FIGURE 15. DC–power module. The DC–power module consists of a 120VAC 40A 2 pole contactor, 1000V–50A full bridge rectifier and two 400VDC–2500uF electrolytic capacitors. By connecting one of the AC input wires to the junction of the two capacitors, the voltage–doubler circuit is made.

Starter Module

The Starter module is a device which creates a high electric potential to ionize the working gas (See Figure 16, 18). Since the ionized working gas is electrically conductive, it starts the arc discharge of the DC–power module. In particular, the ironized gas, which is created to start arc discharge, is called a pilot arc. The starter module consists of an ignition coil, run capacitor, and dimmer switch. The power

source for the starter module is the same AC wall power as for the DC–power module. Sharing the same AC wall power is important because the high voltage, which is generated from the ignition coil, requires a low potential for the return. By sharing the AC wall power, the power module

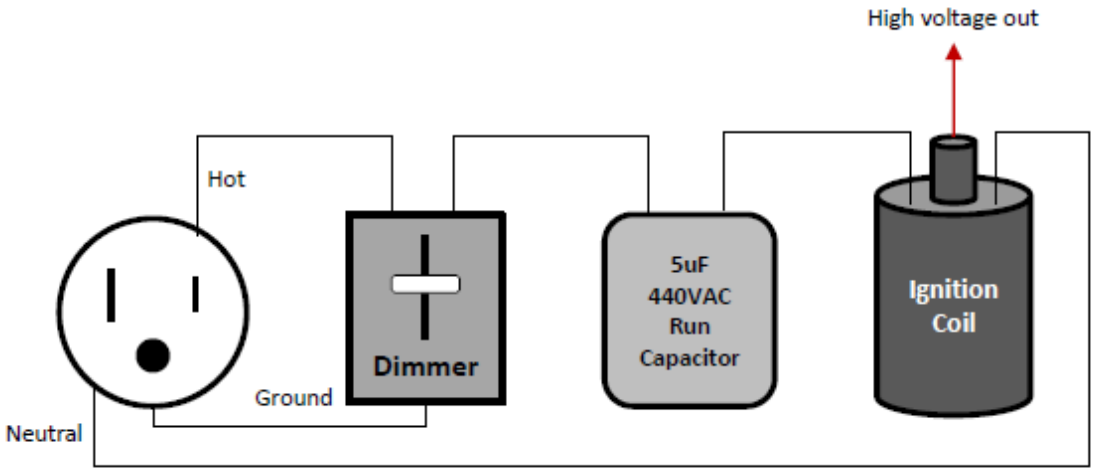

FIGURE 16. Schematic diagram for starter module.

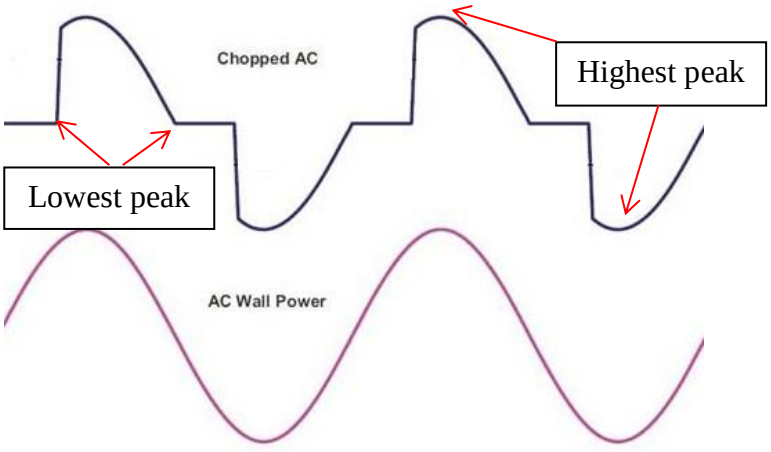

FIGURE 17. The voltage waveform comparison of chopped AC and AC wall power.

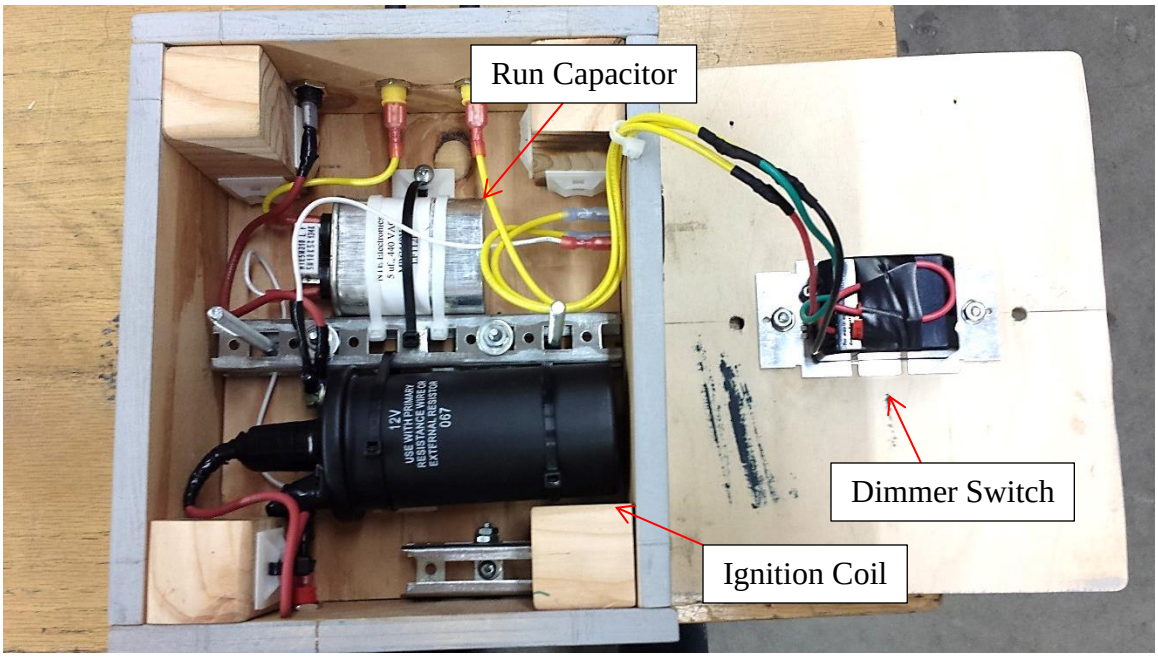

FIGURE 18. Starter module. The starter module consists of a 12V ignition coil, 440VAC–5uF run capacitor, and 600W dimmer switch.

provides the low potential and the starter module takes the cathode for the return. The role of the dimmer switch is to break up the AC sine waves and transform them into near square waves with rounded tops (See Figure 17). The run capacitor is charged up at the highest peak voltage and releases the energy at the lowest peak into the primary coil of the ignition coil. A 440VAC–5uF run capacitor is used to provide enough current for the primary coil and protect the dimmer switch from an inductive kick from the ignition coil. In addition, a 12V Chevy ignition coil is used to convert the low voltage to high voltage.

System Components

System components are devices that control total power consumption and protect electrical components for a reliable operation.

Resistor Bank

The resistor bank consists of two water heater elements (See Figure 19). The main reason of using the water heater element is that it satisfies high power requirements. The maximum rated power and allowable voltage for the water heater element is 5500W and 240V respectively. The resistance of the water heater element is 10 Ω. By using two water heater elements, 5, 10 and 20 Ω resistances are selectable.

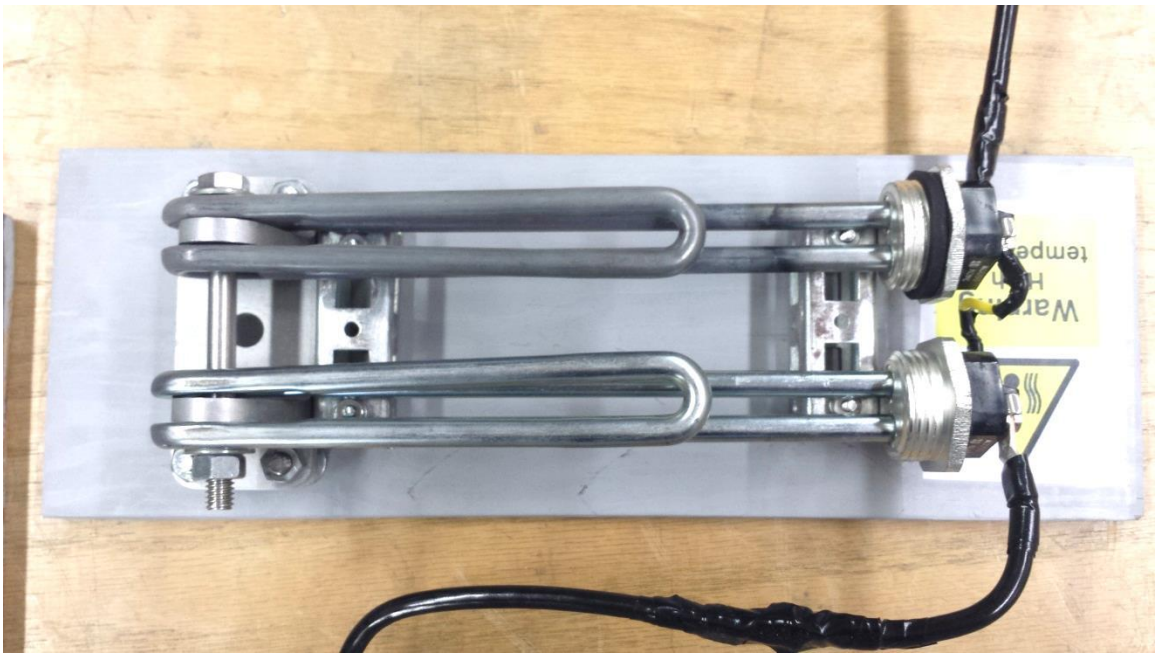

FIGURE 19. Resistor bank. Resistor bank consists of two water heater elements. Each resistance for the element is 10 Ω. 5, 10 and 20 Ω resistances are selectable by changing the wire connection.

Reed Switch Assembly

The reed switch assembly consists of a 200V–1A 10W open reed switch and 14 gauge wires wrapped around it (See Figure 20). The purpose of the reed switch

assembly is to detect the high current as soon as the DC–power module starts to arc and disconnect the starter module. When thermal plasma is being generated, high current flows through the wires and creates a magnetic field. This magnetic field makes contact with two plates in the reed switch and sends 24V to a relay to disconnect the power for the starter module.

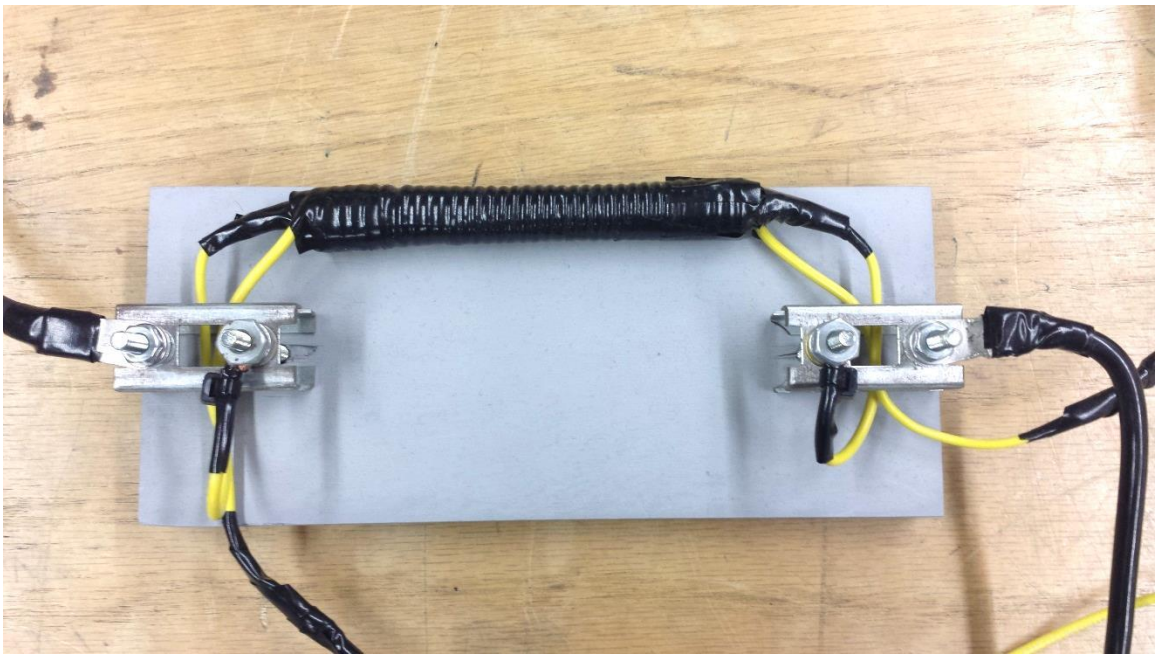

FIGURE 20. Reed–switch assembly. Reed switch assembly consists of a 200V–1A 10W open reed switch and 14 gauge wires wrapped around it.

CHAPTER 4

RESULTS

Test Procedure

The starting conditions of arc discharge and its temperature characteristics are highly dependent on experimental conditions. The factors influencing the arc formation are generally classified into four categories: torch head geometry, type of working gas, gas mass flow rate, and electrical conditions. Since an infinite number of combinations can be made with various parameters, selecting experimental conditions is necessary. For this research, due to test setup constraints, the geometry of the torch head and the type of working gas are fixed. Therefore, mass flow rate and electrical conditions are varied in order to minimize power consumption. Before operating the DC–power module and starter module, electrical conditions must be set first (See Figure 21). The resistance and input voltage are selected by adjusting the wire connection of the resistor bank and the knob position of the variable transformer respectively. After the electrical setting is done, a pressure setting is performed. For the next step, the desired pressure for the upstream (P1) is selected while the solenoid valve is open. When the pressure setup is done, the solenoid valve is closed. After the preset, the test procedure is carried out as follows:

1. Solenoid valve OPEN
2. DC–power module ON

3. Starter module ON

4. Check the presence of arc discharge

5. Record electrical data (Power consumption, voltage, and current)

6. Starter module OFF

7. DC–power module OFF

8. Solenoid valve CLOSE

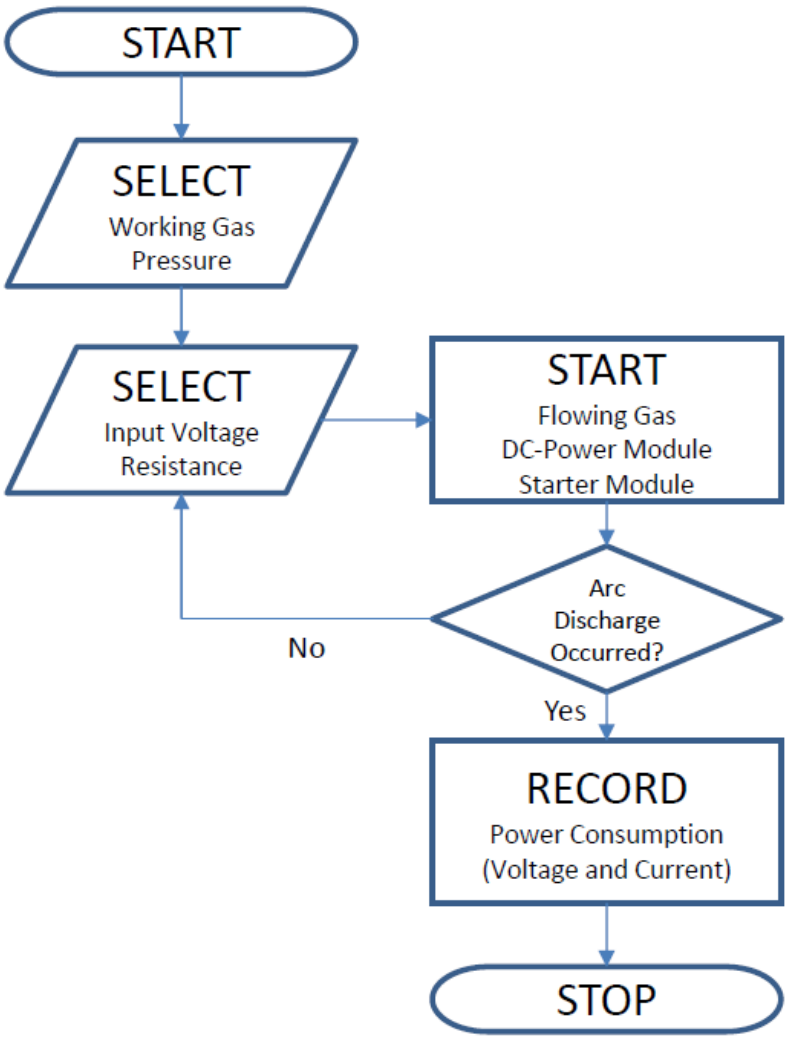

FIGURE 21. Flow diagram for test procedure.

Test Plan

The objective of the test is to find out the output voltage and current that satisfy the minimum power consumption with the given torch head geometries. The pressure setting was made while the solenoid valve was open. 5, 10, and 15 psi were used for the upstream pressure (P1) without involving the plasma drivers. The resistor bank was set to 10 and 20 Ω to control the current. In addition, the variable transformer was set to output voltages from 80 to 120 VAC with 10 VAC voltage gap to control the open circuit voltage and closed circuit voltage for the DC–power module. Therefore, total 30 combinations of the test condition were made. Table 3 and table 4 show the combinations and the results. In addition, digital images for the plasma jet are also taken to check the status of arc discharge and design defects for the torch assembly (See Figure 22, 23).

Measurements

The upstream pressure (P1), downstream pressure (P2) and the current were recorded while arc discharge occurs through the DAQ system. The DC–output voltage from the DC–power module was measured with the Fluke 179 multimeter before and after the arc discharge occurrence. The pressure and current data was not collected when arc discharge did not occur. However, open circuit voltages were recorded to find the condition of the minimum arc–staring voltage. The table 3 and table 4 show the pressures, currents and voltages with 10 and 20 Ω resistance settings respectively. The mass flow rates were calculated based on the pressure difference between P1 and P2. N/A represents the case that the arc discharge did not occur.

TABLE 3. Pressures, Mass Flow Rate, Current and Voltages with 10 Ω Resistance

P1 Gas Flow Only (psi)	P1 Arc Flowing (psi)	P2 Arc Flowing (psi)	Mass Flow Rate (g/s)	VAC Input (Vrms)	Voc Output (VDC)	Vcc Output (VDC)	IDC Output (A)	ID#
5	N/A	N/A	N/A	80	221.0	N/A	N/A	1
	6.208	4.3	0.278	90	248.8	173.9	9.988	2
	6.26	4.419	0.275	100	277.1	188.2	11.119	3
	6.429	4.511	0.284	110	305.0	199.6	12.853	4
	6.543	4.521	0.293	120	332.3	211.3	13.798	5
10	N/A	N/A	N/A	80	221.0	N/A	N/A	6
	10.635	7.744	0.453	90	248.8	177.3	9.380	7
	10.643	7.864	0.445	100	277.1	191.0	10.809	8
	10.75	7.868	0.455	110	305.0	203.9	11.964	9
	10.867	7.842	0.467	120	332.3	214.6	13.128	10
15	N/A	N/A	N/A	80	221.0	N/A	N/A	11
	N/A	N/A	N/A	90	248.8	N/A	N/A	12
	16.199	12.145	0.666	100	277.1	193.4	10.161	13
	16.008	12.538	0.618	110	305.0	205.3	11.824	14
	16.022	12.39	0.631	120	332.3	216.3	13.054	15

Note: Voc and Vcc represent open circuit and closed circuit voltage, respectively. N/A represents the case that the arc discharge did not occur. Refer to Figure 14 for system diagram.

TABLE 4. Pressures, Mass Flow Rate, Current and Voltages with 20Ω Resistance

P1 Gas Flow Only (psi)	P1 Arc Flowing (psi)	P2 Arc Flowing (psi)	Mass Flow Rate (g/s)	VAC Input (Vrms)	Voc Output (VDC)	Vcc Output (VDC)	Current Output (A)	ID#
5	N/A	N/A	N/A	80	221.0	N/A	N/A	16
	N/A	N/A	N/A	90	248.8	N/A	N/A	17
	6.621	4.511	0.301	100	277.1	217.5	6.367	18
	6.71	4.71	0.297	110	305.0	233.4	7.424	19
	6.701	4.686	0.297	120	332.3	248.3	8.221	20
10	N/A	N/A	N/A	80	221.0	N/A	N/A	21
	N/A	N/A	N/A	90	248.8	N/A	N/A	22
	11.25	8.282	0.473	100	277.1	220.4	5.997	23
	11.39	8.244	0.488	110	305.0	236.6	6.991	24
	11.233	8.175	0.478	120	332.3	252.2	7.886	25
15	N/A	N/A	N/A	80	221.0	N/A	N/A	26
	N/A	N/A	N/A	90	248.8	N/A	N/A	27
	N/A	N/A	N/A	100	277.1	N/A	N/A	28
	16.008	12.076	0.653	110	305.0	240.1	6.626	29
	15.724	11.926	0.636	120	332.3	254.6	7.568	30

Note: Voc and Vcc represent open circuit and closed circuit voltage, respectively. N/A represents the case that the arc discharge did not occur. Refer to Figure 14 for system diagram.

Optical Measurements

Visual data is also recorded using a digital camera. The purpose of optical measurements is to record the shape and length of the plasma jet, to then identify design factors of the combustion chamber configuration of a RCS thruster. In addition, the visual data is also helpful to investigate the defects that obstruct the arc formation for the torch head assembly. Figure 22 shows the schematic diagram of the optical measurement setup. A 13–megapixel digital camera was installed on the torch setup. The digital images were taken from both with and without a welding filter glass (Shade 10). Figure 23 shows the comparison between the two different conditions. Due to the high intensity of the light emission, the image of the plasma jet is blurred without a light filter. However, the length of the plasma jet can be estimated through the image with the absence of a filter (See Figure 23). On the other hand, the filtered image shows the more detailed shape of the plasma jet and the higher temperature regions. From the figure 23 (b), the shape of the plasma jet between the tungsten rod and the nozzle is very narrow and constricted; when the plasma jet hits the tungsten rod, it starts to be scattered.

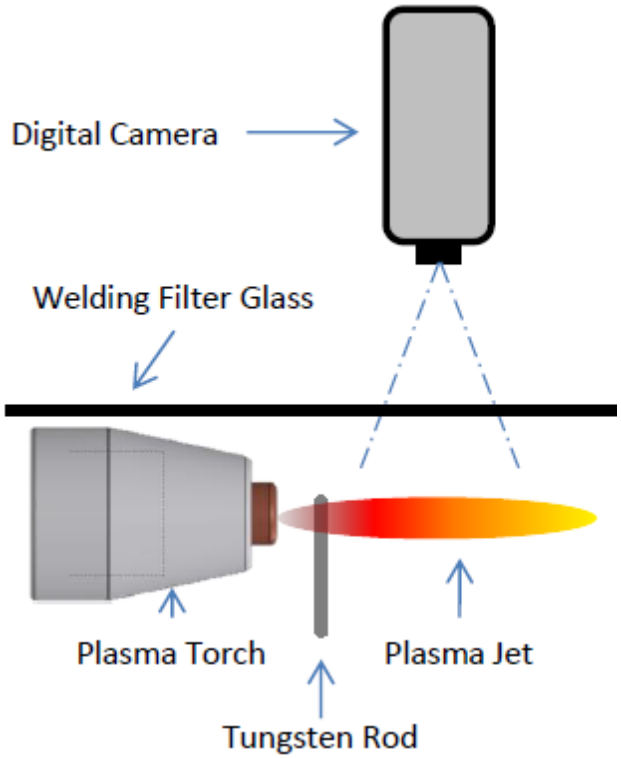

FIGURE 22. Schematic diagram for optical measurement setup. 13–megapixel digital camera was installed on the torch setup. The digital images were taken from both conditions with a filter and without a filter.

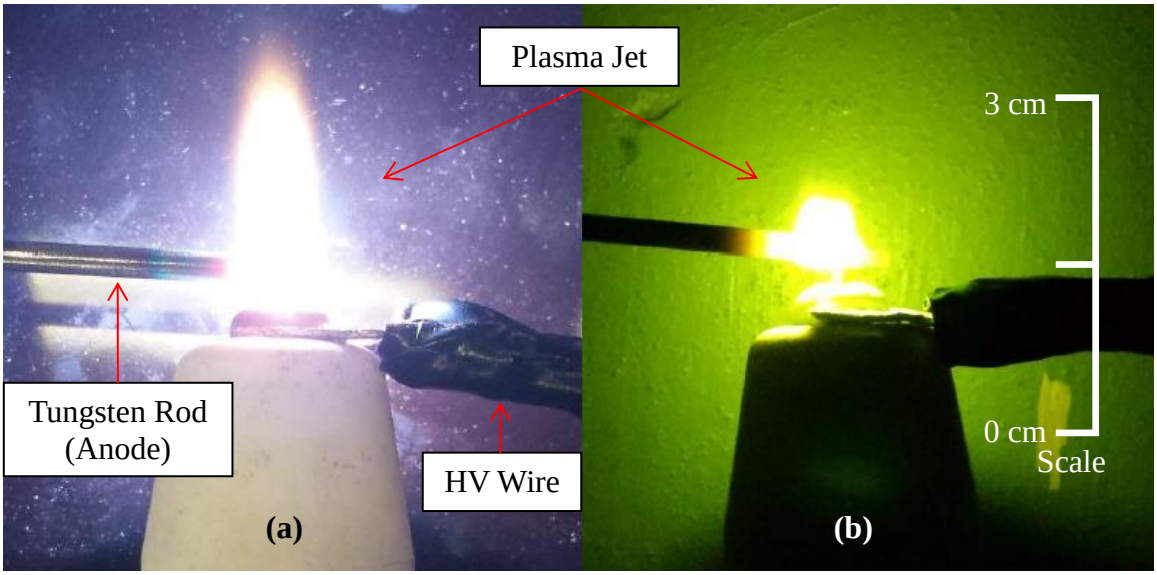

FIGURE 23. The image comparison for plasma jet between the two different conditions. (a) Plasma jet without a light filter and (b) plasma jet with a light filter (Shade 10).

CHAPTER 5

DISCUSSION/ANALYSIS

The test results of the previous chapter show that the minimum open circuit voltage to start arc discharge is 248.8V, with larger values needed when input pressure is increased. The minimum arc–start voltage goes up to 305 V with 20 Ω resistance and 15 psi inaction pressure conditions. The lowest power consumption is 1321 W and table 5 includes the summary of power consumptions for the tests. When comparing 10 Ω and 20 Ω settings, the minimum open circuit voltage was measured as 248.8V and 277.1V, respectively. This result means that a higher resistance setting requires higher voltage to initiate the arc discharge. From the power consumption point of view, on the other hand, the minimum power consumption is recorded as 1,736 W and 1,321 W with 10 Ω and 20 Ω setting, respectively. This result indicates that the lowest open circuit voltage does not guarantee the lowest power consumption. Moreover, higher input pressure tends to make it more difficult to start arc discharge. These results provide tradeoff information between open circuit voltage and power consumption for designing an electrical system for a future plasma igniter.

Temperature Estimation

Determining the temperature of the thermal plasma is highly challenging due to its high temperature. In addition, the temperature profile of plasma jets is changing rapidly after coming out from the nozzle. To analyze the high temperature profile,

spectroscopy is widely used. However, knowing the exact temperature profile is not important for this research and, therefore, normalized power is used to estimate the overall arc temperature. The power consumption and normalized power are calculated and reported in the next section based on the closed circuit voltage and the calculated mass flow rate. According to figure 9, the trend line equation enables finding the estimated arc temperature for the given value of normalized power.

TABLE 5. Temperature Estimation for Plasma Jet based on Normalized Power

ID#	Power (W)	Normalized Power (W ·s/g)	Estimated Temperature (K)	ID#	Power (W)	Normalized Power (W ·s/g)	Estimated Temperature (K)
1	N/A	N/A	N/A	16	N/A	N/A	N/A
2	1,736	6,240	26,309	17	N/A	N/A	N/A
3	2,092	7,592	26,327	18	1,384	4,597	26,286
4	2,565	9,010	26,347	19	1,732	5,833	26,303
5	2,915	9,917	26,359	20	2,041	6,855	26,317
6	N/A	N/A	N/A	21	N/A	N/A	N/A
7	1,663	3,670	26,273	22	N/A	N/A	N/A
8	2,064	4,631	26,286	23	1,321	2,792	26,261
9	2,439	5,357	26,296	24	1,654	3,385	26,269
10	2,817	6,024	26,306	25	1,988	4,153.	26,280
11	N/A	N/A	N/A	26	N/A	N/A	N/A
12	N/A	N/A	N/A	27	N/A	N/A	N/A
13	1,965	2,949	26,263	28	N/A	N/A	N/A
14	2,427	3,923	26,277	29	1,590	2,435	26,256
15	2,823	4,471	26,284	30	1,926	3,025	26,264

Figure 24 indicates that the experimental data from the tests is clustered near the left side of the graph, in a region where the temperature data has not been previously measured. This result suggests that the temperature of plasma may be high (above

25000K) even though the normalized power is low, but the current experimental setup does not allow for verification of this. At the lower normalized power used here, the local temperature may be high, but it is likely to result in the shorter length of plasma jet observed.

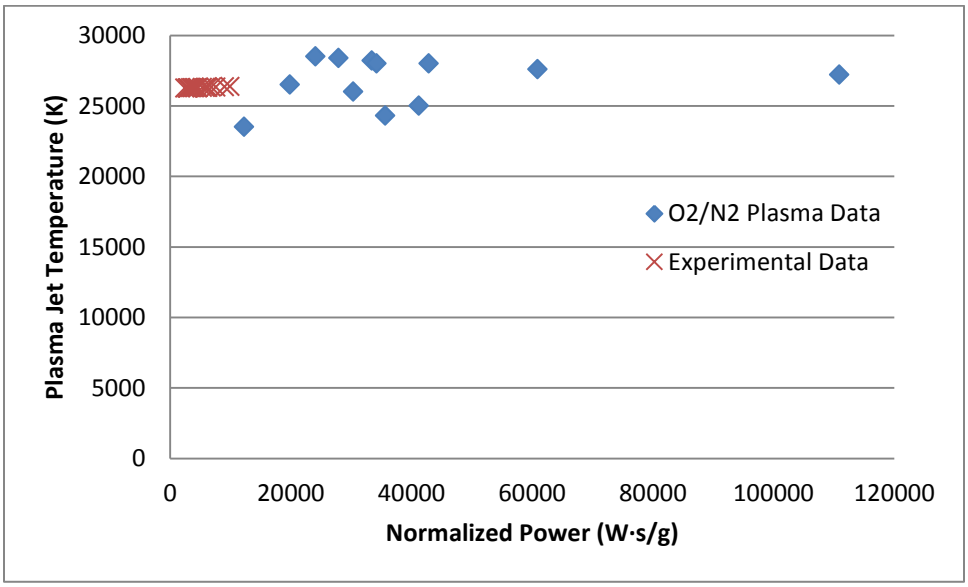

FIGURE 24. O2/N2 plasma temperature vs. normalized power with experimental data.

Input Power Impact on the Mass Flow Rate

As described in chapter 2, an increase in the input power for an arc discharge results in an increase in the chamber pressure with the same mass flow rate. The reason is that the temperature increase creates greater restriction at the throat. However, the throat restriction may also lead to decrease in mass flow rate at the higher temperature. Therefore, it is necessary to investigate the dominating effect between increases in

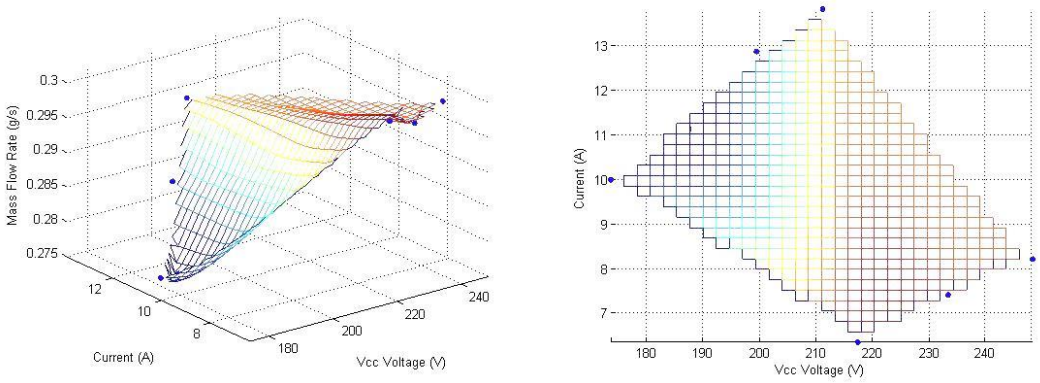

FIGURE 25. Mass flow rate distribution for Vcc voltage and current with 5 psi setting.

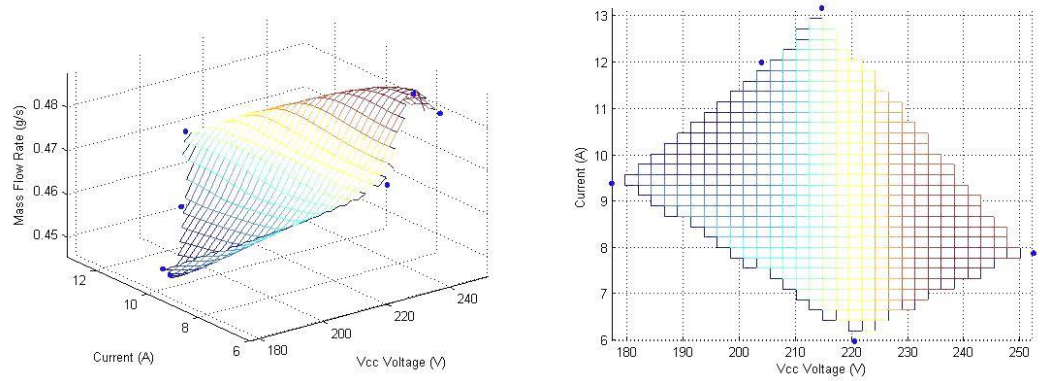

FIGURE 26. Mass flow rate distribution for Vcc voltage and current with 10 psi setting.

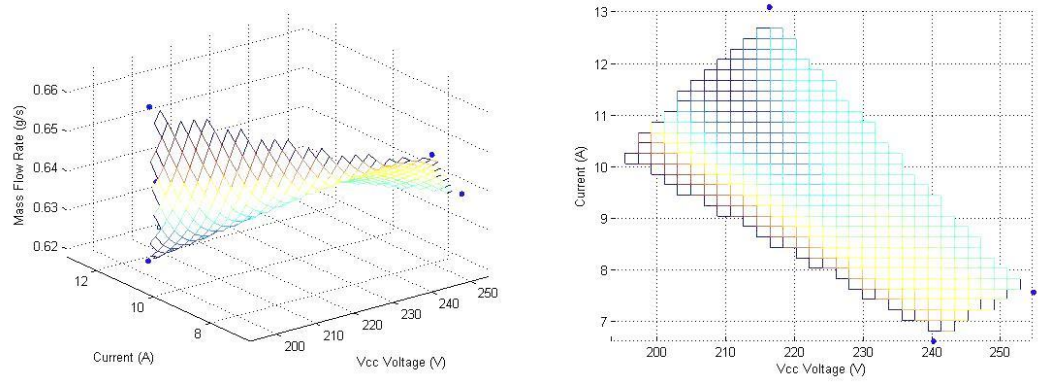

FIGURE 27. Mass flow rate distribution for Vcc voltage and current with 15 psi setting.

chamber pressure and decreases in mass flow rate. This investigation is important because the mass flow rate of working gas has a significant impact on the arc formation and stability. Figures 25–27 show the relationship for the mass flow rate with output voltage and current. The X and Y–axis represent the closed circuit voltage and current respectively. Since the power is the product of the voltage and current, X–Y plane represents the power consumption for the arc discharge. The trend surface analysis is conducted to investigate the mass flow rate change by the power consumption using MATLAB. According to the results, the mass flow rate appears to be decreasing where the current increases. In addition, in the same power consumption, the mass flow rate tends to be higher when the closed circuit voltage is high but the current is low. From these analyses, it can be concluded that the current has a more dominant effect on decreasing the mass flow rate. Since the electrical conditions also change the mass flow rate, a flow controller would be necessary to maintain constant mass flow rates for future research.

Correlation of Pressure and Current

From the previous section, the change of input current appears to lead to a change of mass flow rate. For this section, the upstream pressure (P1), the downstream pressure (P2) and current are plotted to see a more detailed relationship among them. According to figures 28–29, the fluctuation patterns between the downstream pressure (P2) and the current are similar; both current and downstream pressure (P2) lines increase and fall concurrently. 90 and 100 VAC input voltage with 10 Ω and 5 psi (P1) conditions are selected as examples; all other test results also showed similar behaviors.

Therefore, it is proven that the current has a strong relationship with the mass flow rate and the throat restriction.

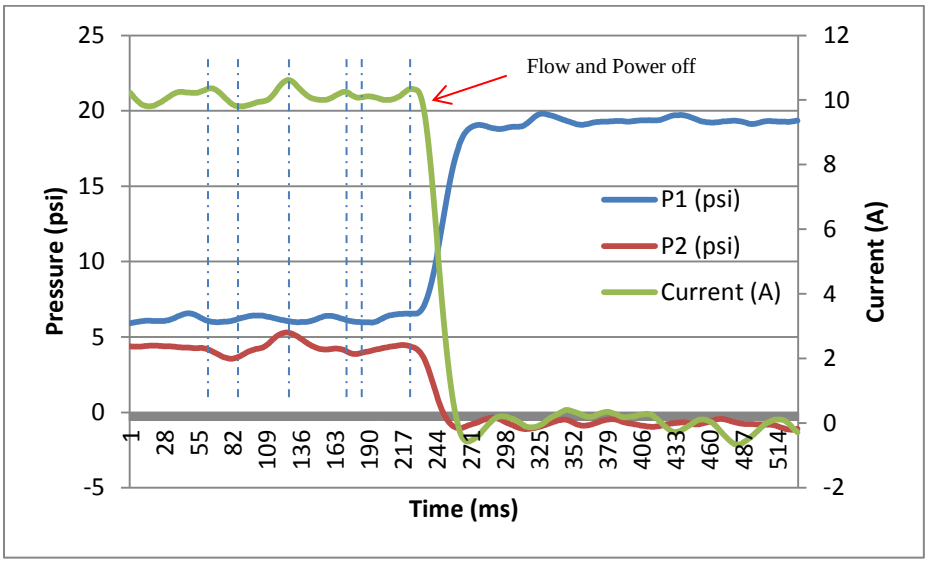

FIGURE 28. Time evolution of pressure and current with 90VAC, 10 Ω and 5 psi setting.

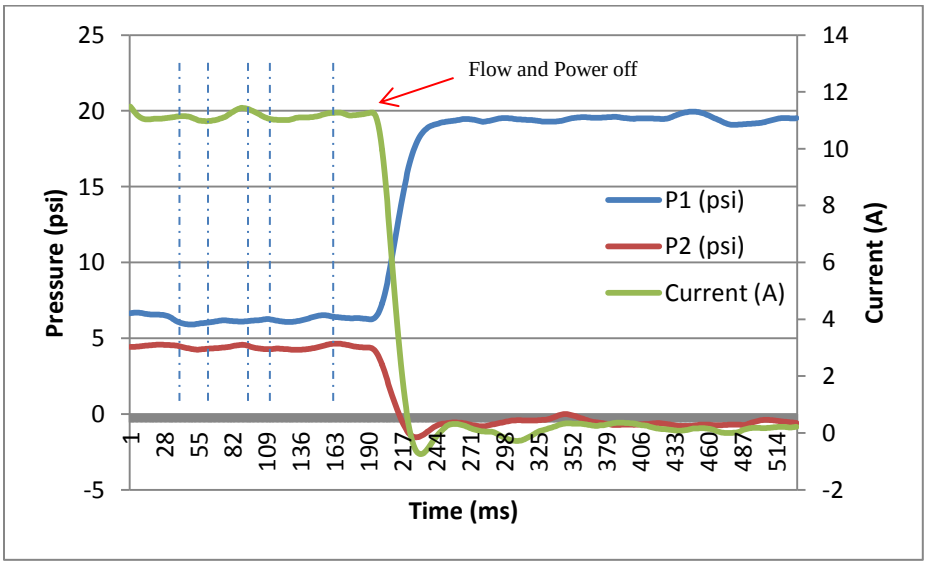

FIGURE 29. Time evolution of pressure and current with 100VAC, 10 Ω and 5 psi setting.

Study of Practical Approaches

The objective of this research is to find the minimum power consumption for arc discharge maintaining its combustion capability. According to the results, the lowest power consumption is 1321 W and the highest power consumption is 2915 W. In addition, the average power consumption is 2060 W from the data. These power consumptions are still high for the actual space vehicle application. The easiest way to reduce the power consumption is by reducing the electrode gap (See Figure 6). Reducing the gap, however, is difficult due to the geometrical limitations. Therefore, determining more advanced approaches may enable the DC–plasma torch to be used as an igniter system for space vehicles. Three approaches (high–power and lightweight energy source, high–frequency and half–duty cycle power system and composite cathode) are proposed as possible solutions.

High–Power and Lightweight Energy Source

Batteries are essential and general power sources for most space vehicles. However, plasma torches consume high power for the operation. Even for this research, the lowest power consumption was recorded as 1321 W. Recent developments in battery technology [26] allow using lithium polymer batteries, which satisfy the high–power and lightweight conditions. Especially, they are able to be operated in higher C–rate (25C–70C) than other batteries. The definition of C–rate is a measure of the current flow when a battery is discharged relative to its maximum capacity; therefore, 1C means that the discharge current can discharge the entire battery in 1 hour. For example, the FlightPower lithium polymer battery (FlightPower LiPo FP70 4S 14.8V 2150mAh) is able to produce 150.5 A with 14.8VDC continuously. Therefore, it has the capability to

supply 2227.4 W for the electrical system. This wattage covers the most power consumptions from this research and the weight of the battery is only 255g. In addition, the duration time for the 1321 W case is 87.2 s for the continuous operation. This duration time indicates that 872 times of RCS operations are possible with the 100 ms plasma igniter operation.

FIGURE 30. FlightPower lithium polymer battery (FP70 4S 2150mAh). Output voltage: 14.8V, capacity: 2150mAh and C–rate for continuous discharge: 70C (150.5A).

High–Frequency and Half–Duty Cycle Power System

According to recent studies [26, 27], pulsed input power with a 50% duty cycle is still capable of producing a thermal plasma while maintaining the operational characteristics. The benefit of the 50% duty cycle is to cut in half the total power consumption, therefore, the scale and technical difficulty of the electrical system development is reduced. Miniaturizing electrical systems is important due to the space and weight limitation for space vehicle. In addition, the battery life can be increased or the weight of the electrical system can be reduced. Figure 29 shows the example waveforms for the 50% duty cycle.

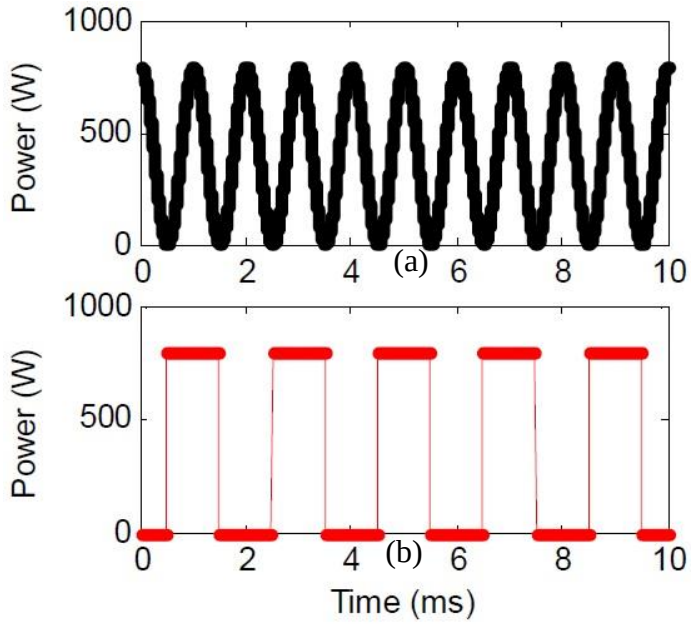

FIGURE 31. Example input power waveforms with 50% duty cycle. (a) Sinusoidal type and (b) square type [26].

Composite Cathode

The cathode material is also an important factor that affects the power consumption and overall characteristic of the arc discharge. A study [28] conducted experiments on the arc discharge characteristics with various composite cathodes and working gases. Pure argon, helium, nitrogen and their mixtures were used for the test at atmospheric pressure. 100 and 150 A currents were used for the electrical condition for arc discharge. The results indicate that Cu-W composite cathode has a better arc stability and lower erosion rate than pure copper. In addition, Cu-Nb composite cathode has much lower erosion rate and much better arc stability than pure copper. Especially, Cu+10%Nb composite cathode has a significant effect on the lowering the arc voltage. The table shows the summary of the test results.

The table 6 shows the arc voltage fraction with different gases. According to the result [28], Cu+10%Nb composite has a small number among all other composite materials for all working gases. Especially, 56% and 36% lower arc voltages are obtained for helium and nitrogen respectively. Therefore, using Cu+10%Nb composite cathode may result in the reduced power consumption.

TABLE 6. Experimental Results for Composite Cathodes with Argon, Helium and Nitrogen Working Gas [28]

	Argon	Helium	Nitrogen
Cu+10%W	0.68	0.53	0.64
Cu+10%Nb	0.59	0.44	0.64
Cu+1.5%Nb	0.96	0.86	

Note: The numbers represent arc voltage (composite) / arc voltage (Cu) with different gases (Cu: Copper, W: Tungsten, and Nb: Niobium).

Conceptual Design of Future Torch Head

The design of PT–31 needs to be transformed to work as a non–transferred type torch. To accomplish the transformation, an anode needs to be incorporated. In addition, a shielding cap should be redesigned as a body structure to hold the other components in place. The design of the nozzle should also be changed to be integrated into the body structure. A cross–sectional scaled diagram of the torch assembly incorporating such features is shown in figure 30. Due to time constraints, this assembly could not be manufactured and tested.

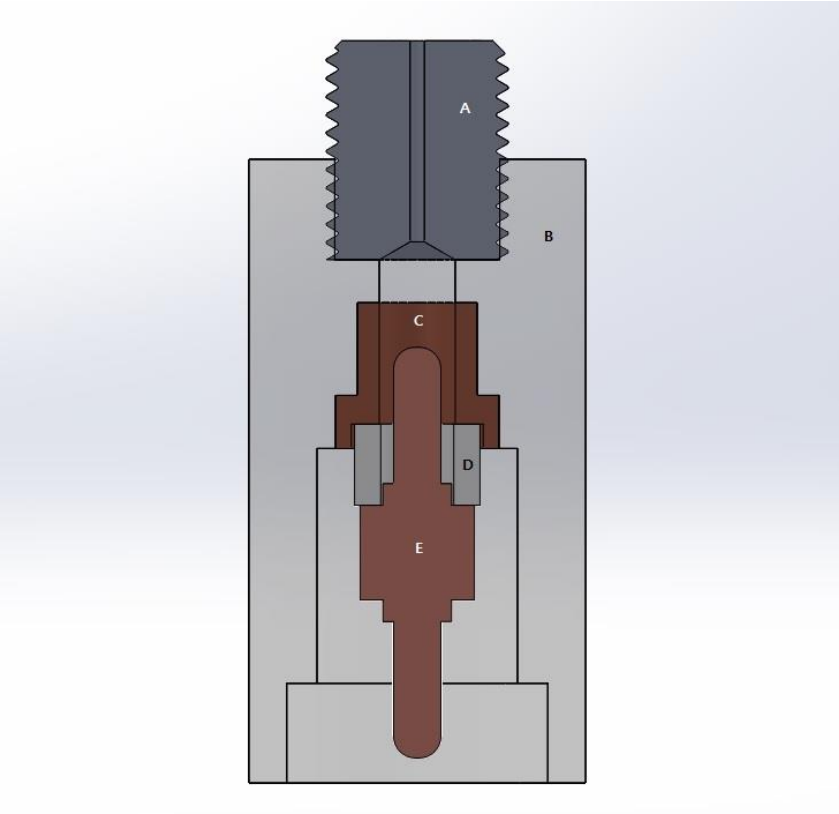

FIGURE 32. Improved torch head assembly design. A: Anode nozzle, B: Body structure, C: High voltage Tip, D: Flow swirler, E: Cathode.

CHAPTER 6

CONCLUSION

A low power DC–thermal plasma torch is investigated as a new approach for igniting RCS thrusters. Arc discharge creates condensed thermal plasma with high temperature characteristics in a small region. By blowing the thermal plasma through a nozzle, making a plasma jet, which is injected into the combustion chamber for RCS thrusters, ignition can be performed. However, the arc formation generally requires high input power and developing the right arc–starting system is essential to initiate the arc discharge. This research focuses on this aspect, which involves plasma generation.

The characteristics of DC–thermal plasma are investigated for low power consumption. A design of an electrical system is presented and studied as a thermal plasma driver. A PT–31 plasma torch head is originally designed as a transferred type, therefore, a conceptual torch design for a non-transferred type head is proposed to work as an igniter for RCS thrusters.

The DC–power module varies the open circuit voltage from 221 V to 332 V for the tests. Resistors of 10 and 20 Ω settings are used to control the current of the thermal plasma. A high voltage starter module is designed to initiate the arc discharge. AC wall power is used for the main power source for both DC–power and high voltage starter modules. For the test procedure, open circuit voltage and flow pressure at P1 need to be set first, and the DC–power module and the starter module need to be turned on next.

When an arc discharge occurs, the data acquisition system records the current and pressure data.

The test results show that the lowest power consumption is 1,321 W with the 10 psi and 20 Ω settings. The lowest open circuit voltage is 248.8 V. However, the lowest power consumption does not correspond to the lowest open circuit voltage. The arc temperature is estimated based on the normalized power and both experimental and theoretical literature data where normalized power refers to the input power per mass flow rate. Data extrapolation suggests that the temperatures of nitrogen thermal plasma are still high (above 25,000 K) even though the normalized power is low. The normalized power, however, does not represent the entire characteristics of the flow field and may result in a shorter length of plasma jet in practical applications. In addition, an increase in input current appears to lead to an overall decrease in mass flow rate. Since the mass flow rate has also a strong connection with power consumption and stability, a flow controller may be necessary for more accurate data collection and analysis. Digital images of plasma jet were taken to verify the shape and length of the plasma jet. The benefits of optical measurements are obtaining useful design factors for combustion chamber geometries and investigating the design defects that obstruct the arc formation for the torch head assembly. Since the tungsten rod appears to disturb the plasma jet, the design of the torch head needs to be refined. The conceptual design of the plasma torch is proposed in chapter 5.

Based on the results and analyses, three approaches (high–power and lightweight energy source, high–frequency and half–duty cycle power system and composite cathode) are proposed as possible solutions for future research. The lithium polymer batteries are

capable of producing high power for a continuous operation and have a high energy to mass ratio. In addition, a 50% duty cycle operation for DC–power module has a possible capability to produce thermal plasma while maintaining the operational characteristics. Lastly, using composite material for the cathode is proposed to reduce the total power consumption. Especially, copper + 10% niobium composite material has a significant advantage for minimizing the power consumption for argon, helium and nitrogen gases.

For future research, a more practical electrical system design and an improved torch head assembly are expected throughout all the possible technical solutions. In addition, combustion tests are necessary to verify the actual functionality of the plasma igniter for RCS thrusters with various oxidizer and fuel mixture ratios. Vacuum tests are also required to prove the operational reliability of the plasma igniter in the space environment.

APPENDICES

APPENDIX A

ELECTRICAL SCHEMATIC FOR PLASMA IGNITER SYSTEM

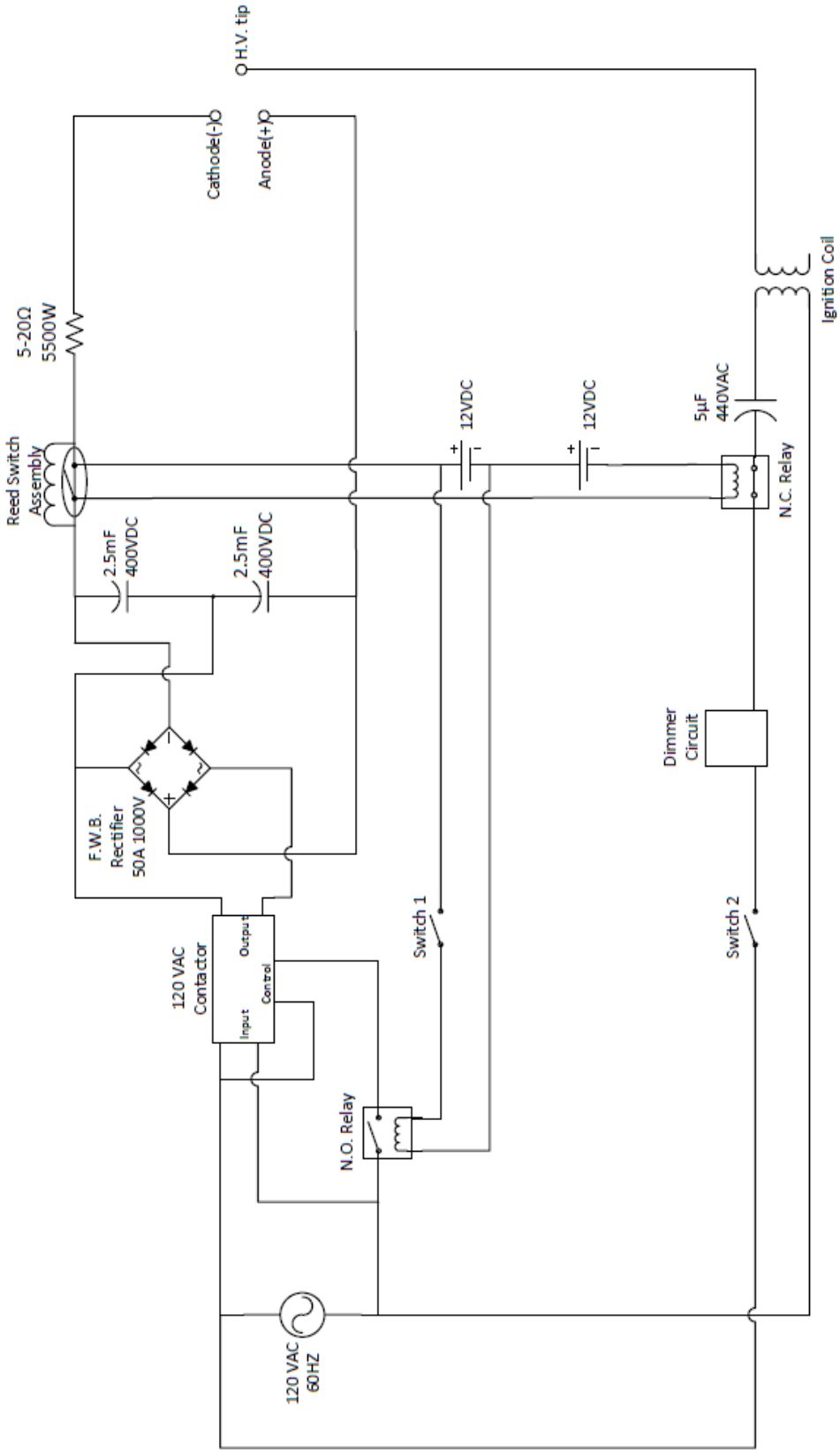

FIGURE 33. Electrical schematic of plasma igniter system.

APPENDIX B

CONCEPT DRAWINGS FOR PLASMA TORCH HEAD

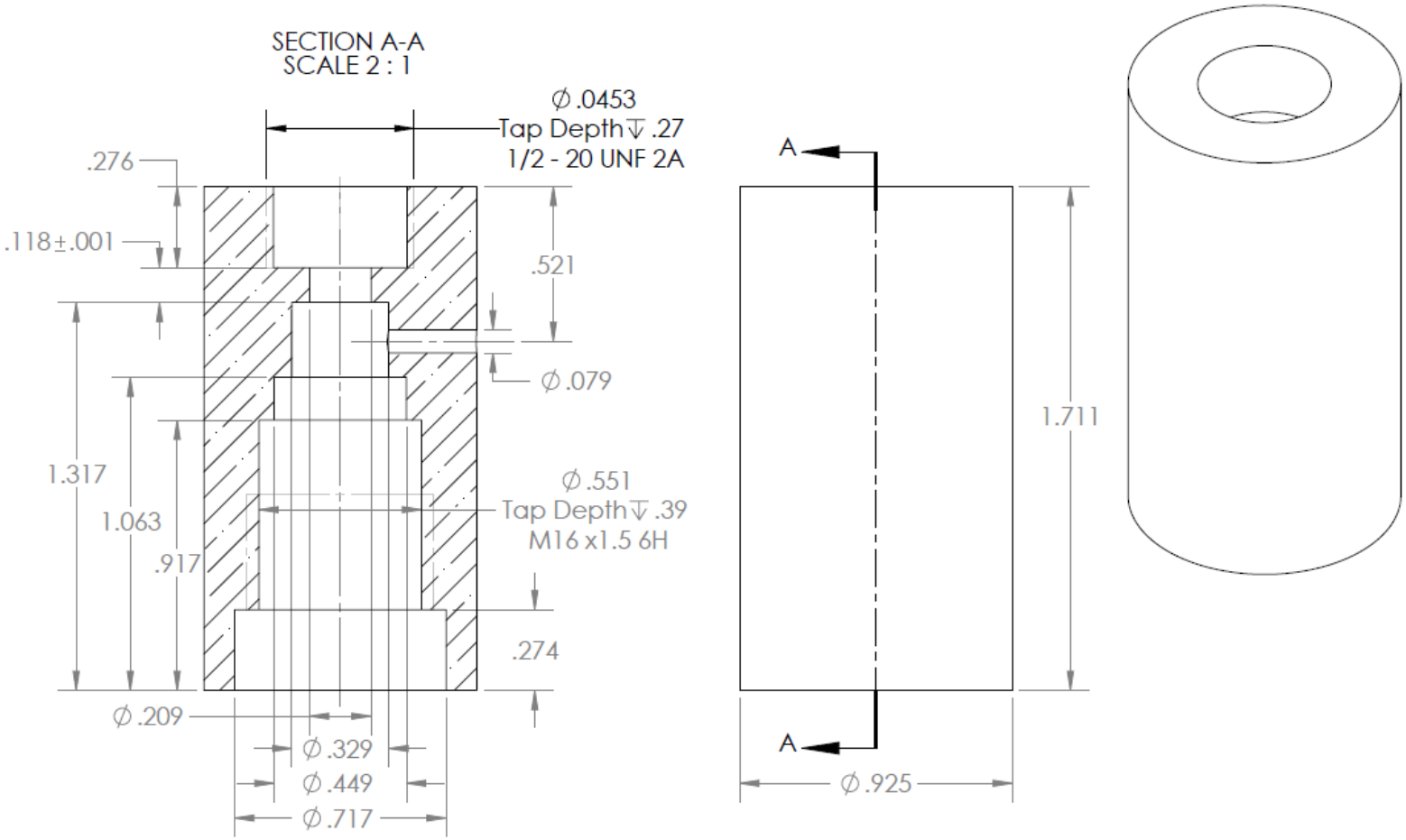

FIGURE 34. Concept drawing for torch body.

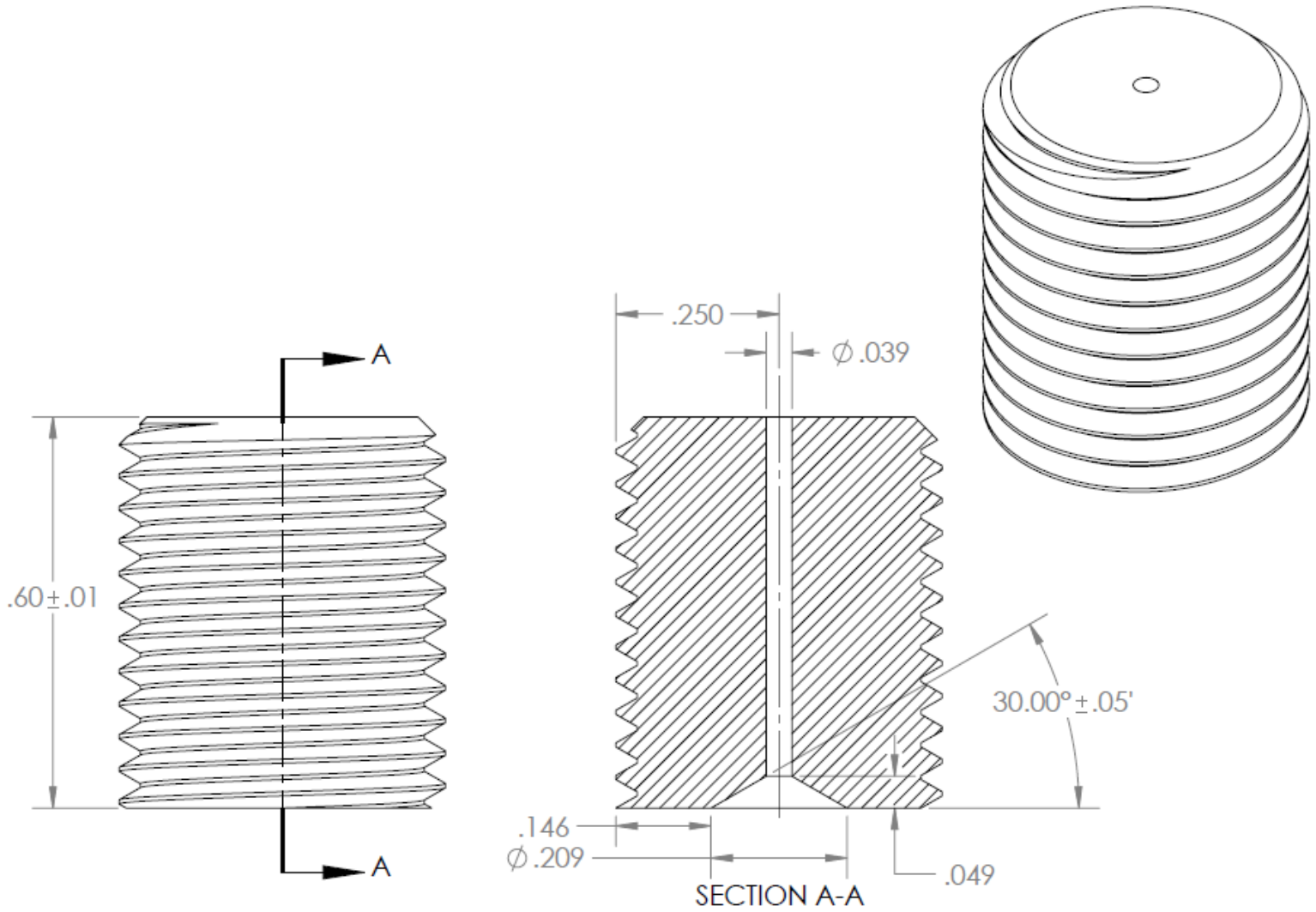

FIGURE 35. Concept drawing for anode.

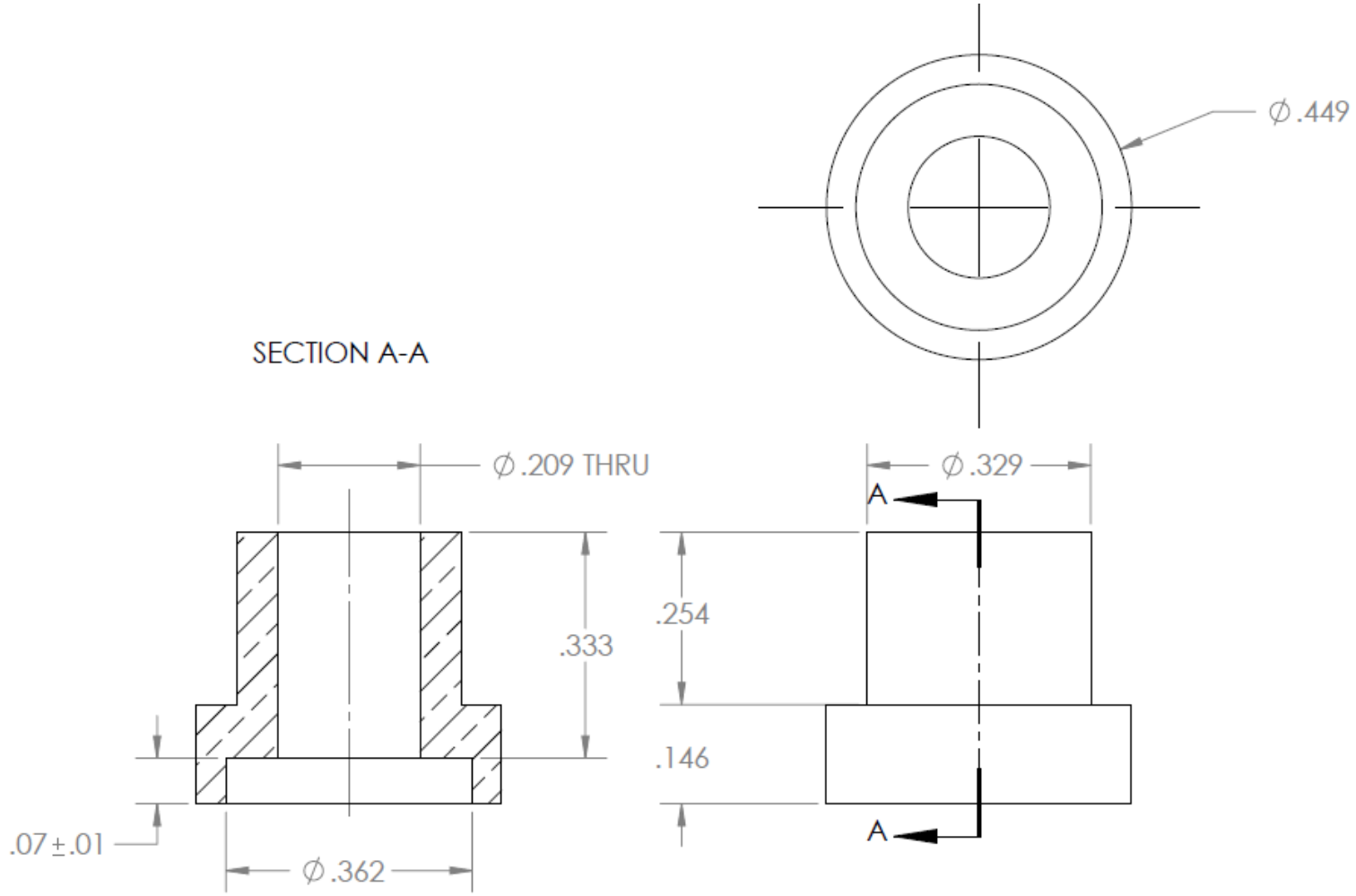

FIGURE 36. Concept drawing for high voltage tip.

REFERENCES

REFERENCES

[1] Federal Aviation Administration, “2014 Commercial Space Transportation Forecasts,” Jul. 15, 2014. [Online]. Available: http://www.faa.gov/about /office_org /headquarters_offices/ast/media/2014_GSO_NGSO_Forecast_Report_FAA_COMSTAC_July_15_2014.pdf. [Accessed: Oct. 3, 2014].

[2] "NASA Completes Altitude Testing of Aerojet Advanced Liquid Oxygen/Liquid Methane Rocket Engine," *Aerojet Rocketdyne*, May 4, 2010. [Online]. Available: http://www.rocket.com/article/nasa-completes-altitude-testing-aerojet-advanced-liquid-oxygenliquid-methane-rocket-engine [Accessed Sept. 18, 2014].

[3] D. Leone, "SpaceX Could Begin Testing Methane-fueled Engine at Stennis Next Year,” *SPACENEWS*, Oct 25, 2013. [Online]. Available: http://spacenews.com/37859spacex-could-begin-testing-methane-fueled-engine-at-stennis-next-year/. [Accessed Sept. 18, 2014].

[4] T. Nagata, J. Torres, J. Culbertson, T. Iizuka, and E. Besnard, "Investigation of Helium Assisted Low Frequency Plasma for Liquid Oxygen and Hydrocarbon Ignition," presented at 47th AIAA/ASME/SAE/ASEE Joint Propulsion Conference & Exhibit, 31 July-03 August 2011, San Diego, California. 2011.

[5] T. Neill, D. Judd, E. Veith and D. Rousar, "Practical uses of liquid methane in rocket engine applications," *Acta Astronautica*, vol. 65, pp. 696–705, Jan. 2009.

[6] K. Breisacher and K. Ajmani, “LOX/Methane Main Engine Igniter Tests and Modeling,” 44th Joint Propulsion Conference, AIAA–2008–4757, July 2008.

[7] K. Breisacher and K. Ajmani, “LOX/Methane Main Engine Glow Plug Igniter Tests and Modeling,” NASA TM-2009-215522, 2009.

[8] I. Toshiaki, E. Besnard and T. Nagata, "Numerical Simulation of LOX/Methane Glow Plug Ignition System," 47th AIAA/ASME/SAE/ASEE Joint Propulsion Conference & Exhibit, 2011, San Diego, California. 2011.

[9] L. S. Jacobsen, C. D. Carter, T. A. Jackson, s. Williams, and J. Barnett, "Plasma-Assisted Ignition in Scramjets," *Journal of Propulsion and Power*. vol. 24, no. 4, July–August 2008.

[10] I. Matveev, S. Matveeva, Y. D. Korolev, O.B. Frants, and N.V. Landl, “A Multi-mode Plasma Pilot”, presented at 45th AIAA Aerospace Sciences Meeting and Exhibit, 8-11 January 2007, Reno, Nevada, 2007.

[11] I. Matveev, S. Leonov, “First Test Results of the Transient Arc Plasma Igniter in a Supersonic Flow”, 3rd International Workshop and Exhibition on Plasma Assisted Combustion, 18-21 September 2007, Falls Church, VA, USA, pp.54-57.

[12] N. Venkatramani, "Industrial plasma torches and applications," *The Indian Academy of Sciences*, vol. 83, no. 3, Aug. 2002.

[13] A. Descoeudres, "Characterization of electrical discharge machining plasmas," Ph.D. thesis, École polytechnique fédérale de Lausanne, Lausanne, EPFL, 2006.

[14] A. Fridman and L. A. Kennedy, *Plasma Physics and Engineering*, New York: Taylor & Francis, 2004, p. 167.

[15] S. D. Gallimore, "A study of plasma ignition enhancement for aeroramp injectors in supersonic combustion applications," Ph.D. dissertation, Virginia Polytechnic Institute and State University, Blacksburg, Virginia, 2001.

[16] J. L Perbola Jr, "Performance of a plasma torch With hydrocarbon feedstocks for use in scramjet combustion," M.S. thesis, Virginia Polytechnic Institute and State University, Blacksburg, Virginia, 1998.

[17] Q. Zhou, H. Li, F. Liu, S. Guo, W. Guo and P. Xu, "Effects of nozzle length and process parameters on highly constricted oxygen plasma cutting arc," *Plasma Chem Plasma Process*, vol. 28, pp. 729–747, Oct. 2008.

[18] R. Huang, H. Fukanuma, Y. Uesugi and Y. Tanaka, "An improved local thermal equilibrium model of DC arc plasma torch," *IEEE Transactions on Plasma Science*, vol. 39, no. 10, pp. 1974 – 1982, Oct. 2011.

[19] G. Li, W. Pan, X. Meng and C. Wu, "Application of similarity theory to the characterization of non-transferred laminar plasma jet generation," *IOPscience Plasma Sources Science and Technology*, vol. 14, pp. 219–225, Feb. 2005.

[20] D. Jing, L. Yaojian, X. Yongxiang and S. Hongzhi, "Numerical simulation of fluid flow and heat transfer in a DC non-transferred arc plasma torch operating under l aminar and turbulent conditions," *IOPscience Plasma Science and Technology*, vol. 13, no.2, pp. 201–207, Apr. 2011.

[21] S. Kim, J. Heberlein, J. Lindsay and J. Peters, "Methods to evaluate arc stability in plasma arc cutting torches," *IOPscience Journal of Physics D: Applied Physics*, vol. 43, pp. 1–11, Dec. 2010.

[22] W. X. Pan, X. Meng, G. Li, Q. X. Fei and C. K. Wu, "Feasibility of laminar plasma-jet hardening of cast iron surface," *Surface and Coatings Technology*, vol. 197, pp. 345–350, Aug. 2004.

[23] S. Ghorui and A. K. Das, "Arc plasma devices: Evolving mechanical design from numerical simulation," *PRAMANA journal of physics*, vol. 80, no. 4, pp. 685–699, Apr. 2013.

[24] J. Eichholz, "How I made my Own plasma cutter from junk," [Online]. Available: http://theplasmacutterman.com/files/The_Plasanator_Plasma_Cutter_Plans_2010.pdf. [Accessed: Sept. 11, 2013].

[25] "Miniature and subminiature solenoid valves," [Online]. Available: ttp://www.farnell.com/datasheets/1673813.pdf. [Accessed: Dec. 3, 2013].

[26] M. A. Peretich, W. F. O'Brien and J. A. Schetz, "Plasma torch power control for scramjet application," Virginia Polytechnic Institute and State University, Blacksburg, Virginia, 2007.

[27] M. Billingsley, D. D. Sanders, W. F. O'Brien and J. A. Schetz, Improved plasma torches for application in supersonic combustion," AIAA Paper 2005-3423, 2005.

[28] R. N. Szente, R. J. Munz and M. G. Drouet, "Electrode materials for plasma torches," *11th International symposium on plasma chemistry, August 22-27, 1993, Loughborough, Leicestershire, England*, 1993. pp. 59-64.